NASA Contractor Report 4171

Thermodynamic Analysis of Compatibility of Several Reinforcement Materials With Beta Phase NiAl Alloys

K. Misra

COOPERATIVE AGREEMENT NCC3-43
NOVEMBER 1988

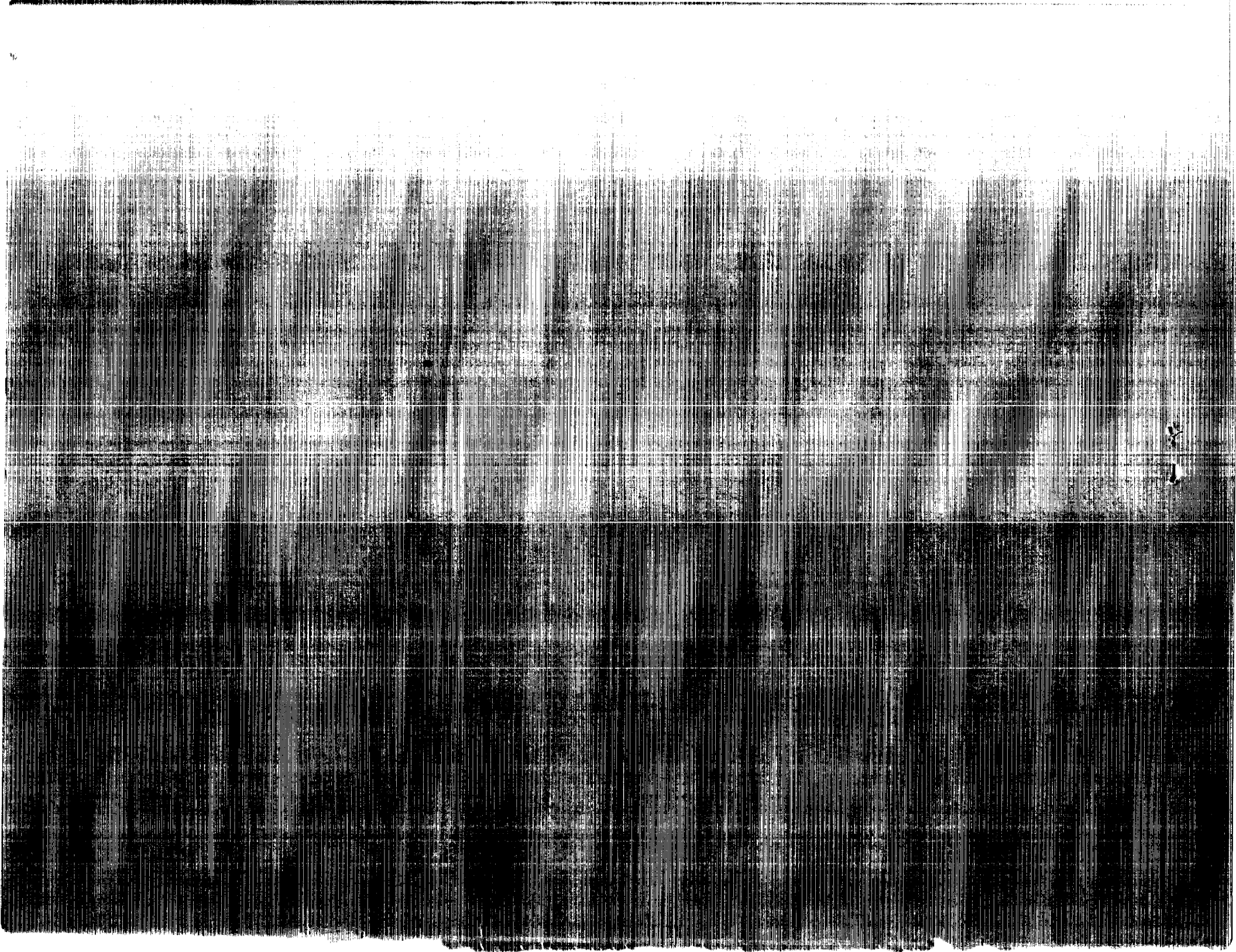

NASA Contractor Report 4171

Thermodynamic Analysis of Compatibility of Several Reinforcement Materials With Beta Phase NiAl Alloys

Ajay K. Misra
Case Western Reserve University
Cleveland, Ohio

Prepared for
Lewis Research Center
under Cooperative Agreement NCC3-43

National Aeronautics
and Space Administration

Scientific and Technical
Information Division

1988

THERMODYNAMIC ANALYSIS OF COMPATIBILITY OF SEVERAL REINFORCEMENT MATERIALS WITH BETA PHASE NiAl ALLOYS

Ajay K. Misra*
Case Western Reserve University
Cleveland, Ohio 44106

SUMMARY

Chemical compatibility of several reinforcement materials with beta phase NiAl alloys within the concentration range 40 to 50 at % Al have been analyzed from thermodynamic considerations at 1373 and 1573 K. The reinforcement materials considered in this study include carbides, borides, oxides, nitrides, beryllides, and silicides. Thermodynamic data for NiAl alloys have been reviewed and activity of Ni and Al in the beta phase have been derived at 1373 and 1573 K. Criteria for chemical compatibility between the reinforcement material and the matrix have been defined and several chemically compatible reinforcement materials have been identified.

INTRODUCTION

Fiber-reinforced intermetallic matrix composites are currently being considered as potential high temperature materials. The choice of a suitable intermetallic matrix is largely a function of the temperature range of interest. Ti3Al- and FeAl-based composites would be suitable for temperatures in the range of 1073 to 1373 K, whereas, NiAl-based systems would be attractive for higher temperatures, i.e. in the range of 1373 to 1673 K. The key factors in the selection of a suitable fiber-reinforcement material are (1) the chemical compatibility of the fiber with the matrix, and (2) close match in thermal expansion coefficient (CTE) between the fiber and the matrix. Thermodynamic-based predictions on chemical stability of the reinforcement material in a given matrix can narrow down the choices for reinforcement materials and thus reduce the experimental effort needed to identify potential reinforcement materials. In this report we examine the chemical compatibility of different reinforcement materials with NiAl alloys from thermodynamic considerations. Keeping in mind the potential temperature range in which NiAl-based composites are likely to be used, all the thermodynamic calculations were made at two temperatures, i.e., 1373 and 1573 K.

THEORETICAL CONSIDERATIONS

Consider the reaction of an intermetallic phase consisting of elements A and B with a reinforcement material consisting of elements C and D. The possible reactions between the intermetallic matrix and the reinforcement material can be grouped under three categories. These are:

(1) Reduction of the reinforcement material by an element of the intermetallic matrix.

---

*NASA Resident Research Associate.

(2) Simultaneous formation of two product compounds by reaction of either one element or both the elements of the intermetallic matrix with the reinforcement material.

(3) Dissolution of the elements of the reinforcement material in the intermetallic matrix.

Besides the above three modes of reactions, it is also possible for dissolution of A and B in the reinforcement material; however, for our calculations the solubility of A and B in the reinforcement material will be assumed to be negligible. In the following, each of the above three modes of reactions will be discussed in detail.

Identification of Possible Stable Product Compounds

For reaction of the intermetallic AB with the reinforcement material CD, the possible product compounds can be identified by examining the phase diagrams for the four binaries: A-C, A-D, B-C, and B-D. Although ternary or higher order compounds are possible, due to the lack of thermodynamic data for ternary compounds, only binary compounds will be considered in the present analysis.

There might be several compounds in a given binary system; however, only those product compounds which are likely to be stable in the alloy matrix will be considered. Therefore the first step in the compatibility calculations is to identify the stable binary product compounds and this will be described in detail. As an example consider the formation of a compound A_xC_y by the reaction

$$xA + yC = A_xC_y \tag{1}$$

for which the equilibrium constant is

$$K_1 = \frac{1}{(a_A)^x \times (a_C)^y} \tag{2}$$

where K_i is the equilibrium constant for the i^{th} reaction and a_i is the activity of element i in the matrix. Assuming unit activity for C, the equilibrium activity of A would be $(1/K_1)^{1/x}$. If the activity of A in the alloy is lower than this value, then the compound A_xC_y is not stable in the alloy and therefore will not be considered in our calculations. Similar calculations can be done for other A-C compounds and the stable product compounds can be identified. Now let us assume that there are several A-C compounds that could be stable in the matrix. For a given activity of A in the matrix we need a certain minimum activity of C for formation of an A-C compound and the compound for which this minimum activity of C has the lowest value will be considered to be the most stable A-C compound in the matrix.

Calculations similar to those described above can be made to identify the most stable product compounds for other three binary system, i.e. A-D, B-C, and B-D binaries. Thus a total of four possible product compounds, two C-containing and two D-containing compounds, can be identified.

In general, it is not necessary to consider all the four product compounds while assessing the compatibility of a given reinforcement material and, as shown below, only two product compounds need to be considered. Let us assume that the four possible product compounds are A_xC_y, A_pD_q, B_iC_j, and B_mD_n. The relative stability of A_xC_y and B_iC_j in the AB matrix are governed by the equilibria for the reaction

$$(j)A_xC_y + (iy)B = (y)B_iC_j + (xj)A \tag{3}$$

for which, assuming unit activity for the compounds B_iC_j and A_xC_y, the equilibrium constant can be written as:

$$K_3 = \frac{(a_A)^{xj}}{(a_B)^{iy}} \tag{4}$$

Thus, for a given a_A and a_B in the alloy, if the activity ratio $[(a_A)^{xj}/(a_B)^{iy}]$ is greater than K_3, A_xC_Y would be the stable compound. On the other hand, if the activity ratio in the alloy is less than K_3, B_iC_j would be the stable product. Similarly, the relative stability of A_pD_q and B_mD_n in the AB matrix is governed by the equilibria for the reaction

$$(n)A_pD_q + (mq)B = (q)B_mD_n + (np)A \tag{5}$$

and if the activity ratio $[(a_A)^{np}/(a_B)^{mq}]$ is greater than the equilibrium constant for the reaction in eq. 5), A_pD_q would be the stable compound in the AB matrix. From the above considerations it becomes evident that only two product compounds, i.e., one from the C-containing group and the other from the D-containing group, need to be considered.

Reduction of the Reinforcement Material

The possible reactions in which one of the alloy components reduces the reinforcement material can be written as:

$$x\underline{A} + yCD = A_xC_y + yD \tag{6}$$

$$p\underline{A} + qCD = A_pD_q + qC \tag{7}$$

$$i\underline{B} + jCD = B_iC_j + jD \tag{8}$$

$$m\underline{B} + nCD = B_mD_n + nC \tag{9}$$

The underline in the above equations denote reduced activities for the elements. The reinforcement material would be considered unstable in the matrix and, therefore, would be incompatible with the matrix if either C or D is formed at unit activity as a result of any of the reactions in eqs. (6) to (9). For reaction products to be formed at unit activity as a result of reactions in eqs. (6) to (9), the first criteria is that the standard Gibbs free energy change ($\Delta G°$) for these reactions must be negative. For reactions with negative $\Delta G°$ values the activity of A or B in the alloy must be greater than certain minimum values as defined below in order for the products to be formed at unit activity.

1. The activity of A (a_A) in the alloy must be greater than $(1/K_6)^{1/x}$ for D to be formed as a result of the reaction in eq. (6).

2. a_A in the alloy must be greater than $(1/K_7)^{1/p}$ for C to be formed as a result of the reaction in eq. (7).

3. The activity of B (a_B) in the alloy must be greater than $(1/K_8)^{1/i}$ for formation of D at unit activity via reaction in eq. (8).

4. a_B in the alloy must be greater than $(1/K_9)^{1/m}$ for formation of C at unit activity via reaction in eq. (9).

Simultaneous Formation of Two Product Compounds

If the calculations show that C and/or D are not formed at unit activity, the next step is to examine if two product compounds can be formed simultaneously via reactions:

$$(qX + py)\underline{A} + (qy)CD = (q)A_xC_y + (y)A_pD_q \quad (10)$$

$$(nx)\underline{A} + (ym)\underline{B} + (ny)CD = (n)A_xC_y + (y)B_mD_n \quad (11)$$

$$(in + jm)\underline{B} + (jn)CD = (n)B_iC_j + (j)B_mD_n \quad (12)$$

$$(jp)\underline{A} + (iq)\underline{B} + (jq)CD = (j)A_pD_q + (q)B_iC_j \quad (13)$$

Again, in order for the products to be formed at unit activity as a result of any of the above reactions, ΔG° for the reaction must be negative. For reactions with negative ΔG° values the following conditions must be satisfied for the above reactions to occur.

1. The activity of A in the alloy must be greater than $(1/K_{10})^{1/(qx+py)}$ for the reaction in eq. (10) to go in the forward direction.

2. The product $[(a_A)^{nx} \times (a_B)^{my}]$ must be greater than $1/K_{11}$ for the reaction in eq. (11) to proceed in the forward direction.

3. The activity of B in the alloy must be greater than $(1/K_{12})^{1/(in+mj)}$ for the reaction in eq. (12) to occur.

4. The product $[(a_A)^{jp} \times (a_B)^{iq}]$ must be greater than $1/K_{13}$ for the reaction in eq. (13) to take place.

The reinforcement material can be considered to be incompatible with the matrix if conditions are sufficient for any of the reactions in eqs. (10) to (13) to occur.

Dissolution of C and D in the Matrix

Now let us consider a situation in which neither D nor C is formed at unit activity as a result either of the reactions in eqs. (6) to (9) nor the conditions are sufficient for the formations of two compounds simultaneously via reactions in eqs. (10) to (13). Now, in order to attain chemical equilibrium

between the matrix and the reinforcement material, the activities of each component must be the same in both the matrix and the reinforcement material. Thus, at equilibrium, the activities of C and D in the alloy must be the same as in the reinforcement phase. Similarly the activities of A and B in the reinforcement phase must be the same as in the alloy. In our calculations it will be assumed that the solubility of A and B in the reinforcement material is small and the physical plus mechanical properties of the reinforcement phase would not be adversely affected by small solubility of A and B in it. Then, only the dissolution of C and D in the AB alloy matrix needs to be considered. The equilibrium conditions for the reaction

$$\underline{C} + \underline{D} = CD \tag{14}$$

dictates that dissolution of C and D in the alloy matrix will continue until the product of their activities, $(a_C \times a_D)$, in the matrix becomes equal to $1/K_{14}$. The equilibria for the reaction in eq. (14) gives only the product of the equilibrium activities of C and D but not the individual activities of C and D. However, as described below, the minimum values for equilibrium a_C and a_D in the matrix can be calculated.

Since the activities of the elements C and D in the matrix are related by the equilibria for the reaction in eq. (14), the minimum activity of one of these elements can be calculated if we can determine the maximum possible value for the activity of the other. As an example consider a situation in which we wish to calculate the minimum activity for the element D in the matrix. This requires determination of the maximum value of a_C in the matrix. If it is known that a compound A_xC_y can be formed in the binary system A-C, then element C will continue to dissolve in the matrix and thus gradually increase its activity until the activity becomes equal to $[K_1 \times (a_A)^x]^{-1/y}$. When the activity of C becomes equal to $[K_1 \times (a_A)^x]^{-1/y}$, the compound A_xC_y precipitates out, and the matrix becomes saturated with C. This activity of C at which precipitation of A_xC_y occurs would be the maximum possible value for the activity of C in the matrix and can be denoted as $(a_C)_{max}$. As stated earlier, the activities of C and D in the matrix are related by the equilibria expression for the reaction in eq. (14) and, therefore, the activity of D corresponding to $(a_C)_{max}$ is the minimum possible value for a_D in the matrix and is equal to $1/[K_{14} \times (a_C)_{max}]$. Since the combination of the reactions in eqs. (1) and (14) lead to the reaction in eq. (6), the minimum value for the activity of D in the matrix, denoted as $(a_D)_{min}$, would simply be the equilibrium a_D calculated from the equation:

$$K_6 = (a_D)^y/(a_A)^x \tag{15}$$

Similarly, if instead of A_xC_y, B_iC_j is determined to be the stable C-containing compound in the matrix, $(a_D)_{min}$ would be the equilibrium a_D for the reaction in eq. (8), which is:

$$K_8 = (a_D)^j/(a_B)^i \tag{16}$$

If none of the intermediate compounds in either A-C or B-C binaries are stable in the alloy matrix or if there are no intermediate compounds in either of these binaries, then the minimum equilibrium value for a_D can be calculated from the equilibria for the reaction in eq. (14) by assuming the activity of C to be unity, i.e., $(a_D)_{min} = 1/K_{14}$.

For situations in which the principal mode of interaction between a reinforcement material and the matrix is dissolution of C and D in the matrix, two numbers need to be considered while assessing the compatibility of the reinforcement material with the matrix. These are the minimum values for a_C and a_D in the matrix. It is somewhat difficult to specify any number for $(a_D)_{min}$ or $(a_C)_{min}$ below which the reinforcement material would be considered compatible with the matrix. While assessing the compatibility of a given reinforcement material, several factors including the solubility of D and C in the matrix AB and the level of D and C that can be tolerated in the matrix without adversely affecting the composite performance should be considered. For example, consider a situation in which the $(a_D)_{min}$ is calculated to be 0.8, however, the solubility of D in the AB matrix is very low (on the order of 1 to 10 ppm). In such a situation, even if the calculated $(a_D)_{min}$ is relatively high, the reinforcement material would still be compatible with the matrix. Now consider another situation where $(a_D)_{min}$ is calculated to be 10^{-5} and the solubility of D in the AB matrix is fairly high. Furthermore, let us assume that there is strong negative interaction between D and the elements A and B in the matrix and the activity coefficient of D in the solid solution is on the order of 10^{-3}. Since activity = activity coefficient x mole fraction, the equilibrium mole fraction of D is calculated to be 0.01. Thus, at equilibrium the matrix will contain 1 mol % D and the question should be asked if this level of D in the matrix would adversely affect the performance of the composite. If the answer is "yes," the reinforcement material would then be considered incompatible with the matrix.

Since thermodynamics of many ternary systems A-B-C and A-B-D are not known, it is somewhat difficult to predict on the basis of the calculated values for $(a_C)_{min}$ and $(a_D)_{min}$ whether or not a reinforcement material would be compatible with the matrix. However, in general, it can be qualitatively said that the lower the calculated values for $(a_C)_{min}$ and $(a_D)_{min}$ are, the greater will be the extent of compatibility of the reinforcement material with the matrix. In our calculations, if the calculated values for $(a_C)_{min}$ and $(a_D)_{min}$ are less than 10^{-3}, the reinforcement material will be considered to be compatible with the matrix. It must be remembered that the number 10^{-3} for $(a_C)_{min}$ and $(a_D)_{min}$ is clearly an arbitrary one and is set merely for screening of different reinforcement materials. If $(a_C)_{min}$ and $(a_D)_{min}$ are calculated to be less than 10^{-3}, the reinforcement material/matrix combination can be taken for further analysis and experimentation.

SUMMARY OF CALCULATION PROCEDURES

A summary of the sequence of steps required to determine the compatibility of an intermetallic matrix AB with a reinforcement material CD is given below.

1. Identify the intermediate compounds in the binaries A-C, B-C, A-D, and B-D. If there are no product compounds in any of the binaries, then go to step 5.

2. For a given matrix composition determine the most stable C-containing and D-containing compound in the matrix.

3. Determine if conditions are satisfied for any of the reactions in eqs. (6) to (9) to occur leading to the formation of either C or D at unit activity. If C or D are formed at unit activity as a result of any of these

reactions, then the reinforcement material is not compatible with the matrix and further calculations are not necessary.

4. Determine if conditions are satisfied for simultaneous formation of two product compounds at unit activity by any of the reactions in eqs. (10) to (13). If so, then the reinforcement material is not compatible with the matrix and further calculations are not necessary.

5. Calculate the minimum possible values for a_C and a_D in the matrix.

MATRICES AND REINFORCEMENT MATERIALS

The matrices considered in the present study are alloys within the β' NiAl phase with concentrations ranging from 40 to 50 at % Al. The reinforcement materials considered in the present study include carbides, oxides, borides, nitrides, silicides, and Be-rich intermetallic compounds. A list of the reinforcement materials considered in the present study is shown in table I.

THERMODYNAMICS OF NiAl SYSTEM

The NiAl phase diagram, taken from reference 1, is shown in figure 1. In the present analysis, only β' NiAl phase will be considered. The thermodynamic activity of Al in the NiAl system have been measured by Steiner and Komarek (ref. 2) by an isopeistic method and their activity data at 1273 K are shown in figure 2. There is a sharp increase in the activity of Al over the concentration range 48 to 50 at % Al, with the most rapid rise in activity occurring at 49 at % Al. Drastic change in activities over a very narrow concentration range is indicative of strong ordering in the system and the composition at which the most rapid change in activities occur represent the state of maximum order. Normally the highly ordered structure in an alloy system corresponds to the intermediate phase at the stoichiometric composition and, therefore, the equimolar Ni-50Al composition should exhibit the maximum degree of order in the β' phase. The enthalpy of mixing data of Henig and Lukas (ref. 3) for the NiAl system show a sharp minima at the equimolar composition, further confirming that Ni-50Al has the most ordered structure in the β' phase. Thus, the most rapid increase in the Al activity in the β' phase should occur at 50 at % Al instead of 49 at % Al as obtained from Steiner and Komarek's data. Libowitz (ref. 4) and Neumann et al. (ref. 5) have analyzed the relationship between the point defects and thermodynamic properties for the β' NiAl phase and have suggested that there might have been a systematic error in composition in Steiner and Komarek's study. Based on the fact that the maximum ordering in the β' phase should occur at 50 at % Al, Libowitz and Neumann et al. suggest that corrections should be made to the compositions in Steiner and Komarek's data such that the most rapid rise in Al activity occurs at 50 at % Al.

In the present analysis a smooth curve is drawn through the data points in figure 1 and 1 at % Al is then added to all the compositions so that the most rapid increase in Al activity occurs at the equimolar composition. The corrected activity curve is shown in figure 3. The activity values shown in figure 3 are with respect to liquid Al as the standard reference state. Activities with respect to solid Al can be obtained via

$$RT \ln a_{Al}^{s} = RT \ln a_{Al}^{l} + \Delta G_{Al}^{fus} \qquad (17)$$

where a_{Al}^{s} and a_{Al}^{l} are activities of Al with respect to solid Al and liquid Al, respectively, as the standard reference state; ΔG_{Al}^{fus} is the Gibbs free energy of fusion of Al.

Hanneman and Seybolt (ref. 6) performed Gibbs-Duhem integration of Steiner and Komarek's Al activity data to obtain the activities of Ni in the NiAl system. Ni activity values based on Gibbs-Duhem integration of Steiner and Komarek's Al activity data are also reported in the compilations by Hultgren et al. (ref. 7). Since the above mentioned authors did not make any corrections to Steiner and Komarek's Al activity data, the derived Ni activities will be in error, the error being significant in the concentration range in which drastic change in activities occur, i.e., in the range of 48 to 52 at % Al. Therefore in the present study the nickel activities were derived by performing Gibbs-Duhem integration on the corrected Al activity data shown in figure 3. The calculated activities of Ni at 1273 K along with the corrected values for the activity of Al (with respect to solid Al as the standard reference state) in the β' phase as a function of composition are shown in table II.

Since composites based on β' NiAl are targeted for applications in the temperature range of 1373 to 1673 K, the activity data in table II need to be extrapolated to higher temperatures. Such extrapolations can be done via equations

$$\log(a_{Al})T_2 - \log(a_{Al})T_1 = \frac{\Delta\bar{H}_{Al}}{4.575}\,(1/T_2 - 1/T_1) \tag{18}$$

$$\log(a_{Ni})T_2 - \log(a_{Ni})T_1 = \frac{\Delta\bar{H}_{Al}}{4.575}\,(1/T_2 - 1/T_1) \tag{19}$$

where $\Delta\bar{H}_{Al}$ and $\Delta\bar{H}_{Ni}$ are the partial molar enthalpies of Al and Ni, respectively, in the NiAl phase; T_1 and T_2 are two different temperatures. The partial molar enthalpies for Ni and Al, shown in figure 4, were derived from the integral enthalpy of mixing data of Henig and Lukas (ref. 3). The partial molar enthalpies are constant for both positive and negative deviations from the stoichiometric (equimolar) composition, changing rapidly from one to the other at the stoichiometric composition. The partial molar enthalpy at the stoichiometric composition will be taken to be the average of the two values corresponding to the negative and positive deviations from the stoichiometric composition. The calculated activities of Ni and Al at 1373 and 1573 K are given in tables III and IV. All the compatibility calculations for the NiAl alloys will be performed at these two temperatures only.

Because of considerable degree of experimental scatter in Steiner and Komarek's original data (see fig. 1), there is some degree of uncertainty in the activity values given in tables II to IV, the uncertainties being greater in the concentration range in which there is drastic change in activities of the components. Clearly, much needs to be done to determine the activities in the NiAl system, particularly at compositions closer to the stoichiometric NiAl composition.

THERMODYNAMIC DATA FOR COMPOUNDS

Appendix A gives the Gibbs free energy of formation (ΔG°_{f}) of different compounds at 1373 and 1573 K. Unless otherwise stated, most of the thermodynamic data were taken either from JANAF Thermochemical tables (ref. 8) or from the compilations by Barin and Knacke (ref. 9). The Gibbs energies of formation data for many intermetallic compounds are not available and for such compounds, if enthalpy of formation data at 298 K are available, Gibbs energy of formation is assumed to be the same as the enthalpy of formation at 298 K (ΔH°_{298}). If Gibbs energy of formation data are available only at one temperature, then the same value is assumed at other temperatures. The Gibbs energies of formation for compounds containing elements with low melting points like Al, Ca, La, and Mg are derived with respect to solid as the standard reference state for these elements. The Gibbs energies of formation for Ni_2Si and NiB compounds have been estimated in this study and the estimation procedure will be discussed in appendix B.

POSSIBLE STABLE PRODUCT COMPOUNDS IN THE MATRIX

The possible binary product compounds that are likely to be stable as a result of interaction of the intermetallic matrix with elements of the reinforcement materials considered in this study are given in appendix C.

RESULTS AND DISCUSSION

The reinforcement material is considered to be not compatible with the matrix if (1) conditions are sufficient for any of the reduction reactions to occur, or (2) conditions are sufficient for simultaneous formation of two product compounds. If the calculations show that dissolution of elements of the reinforcement material (C and D) in the matrix is the predominant mode of reaction between the alloy and the reinforcement material, then $(a_C)_{min}$ and $(a_D)_{min}$ values are considered to be high if they are greater than 10^{-3}, otherwise they are considered low. If $(a_C)_{min}$ and $(a_D)_{min}$ are high and it is known that there is significant solubility of C and D in the matrix, then the reinforcement material is considered to be incompatible with the matrix. On the other hand, if the calculated values for $(a_C)_{min}$ and $(a_D)_{min}$ are high but the solubility of C and D in the NiAl matrices are not known, it will be indicated that the compatibility would depend on solubility of C and D in the matrix.

A summary of the results of our thermodynamic calculations are given in tables V to X which indicate the principal mode of reaction between NiAl alloys and the reinforcement materials and comments regarding the compatibility of a given reinforcement material. For situations in which the principal mode of reaction between the reinforcement material and the intermetallic matrix is dissolution of the elements of the reinforcement material in the matrix, tables V to X would indicate whether the minimum values for the activities of these elements in the matrix are high or low, i.e. whether the activities are greater than 10^{-3} or not. The exact values for these activities as a function of alloy composition and temperature are given in appendix D.

Compatibility with Carbides

In this section Me and C stand for the metallic element of the carbide and carbon, respectively. For alloys with lower Al concentrations (<45 at % Al), $(a_C)_{min}$ is high for all the carbides except for TiC and thus the compatibility of other carbides would depend on the solubility of C in the matrix. TiC appears to be the only carbide that is compatible with all alloys within the concentration range 40 to 50 at % Al. On the other hand, there are many carbides which would be compatible with NiAl alloys near the equiatomic composition. These are HfC, NbC, TaC, Ta_2C, TiC, and ZrC. Table XI shows these carbides in order of decreasing values for $(a_{Me})_{min}$ and $(a_C)_{min}$ in the matrix at 1573 K. Only those carbides for which $(a_{Me})_{min}$ and $(a_C)_{min}$ are calculated to be less than 10^{-3} are listed in this table. As shown in table XI, HfC is determined to be the most stable carbide for the alloy Ni-50Al at 1573 K. TiC and ZrC would also be very stable for Ni-50Al at 1573 K.

In summary, HfC, TiC, and ZrC appear to be the best choices as reinforcement material among all the carbides for alloys near the equiatomic composition. On the other hand, TiC would be the best choice for alloys with lower Al concentrations.

Compatibility with Borides

HfB_2, TiB_2, and ScB_2 are the only three borides that are likely to be compatible with NiAl alloys with lower Al concentrations (<45 at % Al) at both the temperatures, i.e., 1373 and 1573 K. There are several borides that are likely to be compatible with NiAl alloys near the equiatomic composition. A list of these borides in order of decreasing activities for $(a_{Me})_{min}$ and $(a_B)_{min}$ (Me and B stand for metallic element and boron, respectively in the compound Me_xB_y) in the matrix at 1573 K are given in table XII. HfB_2, TiB_2, and ScB_2 are the most stable borides in Ni-50Al matrix at 1573 K. Since these three borides are also the only ones that are compatible with NiAl alloys having lower Al concentrations, they appear to be the best choices among all the borides for reinforcement with NiAl alloys.

Compatibility with Oxides

Because of very small solubility of atomic oxygen in NiAl alloys, dissolution of atomic oxygen in NiAl alloys is not considered while determining the compatibility of oxides with NiAl alloys. The oxides Al_2O_3, BeO, Gd_2O_3, HfO_2, La_2O_3, Sc_2O_3, and Y_2O_3 are determined to be compatible with all NiAl alloys within the concentration range 40 to 50 at % Al. Ranking of the compatibility of these oxides with Ni-50Al alloy at 1573 K in order of decreasing activities for $(a_{Me})_{min}$ in the matrix is given in table XIII. The same rankings also hold good for other compositions.

ZrO_2 is determined to be compatible with alloys having alloy concentrations greater than 42 at %, but it may not be a suitable reinforcement material because of a phase transformation at 1478 K. However, ZrO_2-containing compounds or ZrO_2 stabilized by adding other oxides would have potential as reinforcement materials. Also, in mixed oxides ZrO_2 would be at a reduced activity which might make it compatible with lower Al-containing alloys. Few mixed oxides like $Al_2O_3.ZrO_2$ and $Y_2O_3.2ZrO_2$ might be promising as potential

reinforcement materials. CaO is compatible with NiAl alloys having Al concentrations less than 49 at %, but may not be compatible with Ni-50Al. However, a mixed oxide compound containing CaO such as $CaZrO_3$ might be compatible with Ni-50Al because of lower CaO activity in this compound. Also, ZrO_2 partially or fully stabilized by CaO additions is likely to be compatible with NiAl matrices.

Magnesium oxide (MgO) would not be compatible with NiAl alloys if both reinforcement material and the matrix are exposed to a dynamic environment because of evaporation of Mg from the system. However, since the solubility of Mg in NiAl matrices are likely to be very small, MgO would be compatible with NiAl alloys if the reinforcement material is completely enclosed inside the matrix.

Compatibility with Nitrides

Dissolution of atomic nitrogen in NiAl alloys is not considered for calculations on compatibility of nitrides with the alloys. There is no reaction between NiAl alloys and AlN and therefore AlN would be the most stable reinforcement material in NiAl matrices. Among other nitrides, HfN, TiN and ZrN are determined to be compatible with all NiAl alloys within the composition range 40 to 50 at % Al. Table XIV ranks these three nitrides with regards to compatibility with Ni-50Al at 1573 K in order of decreasing values for $(a_{Me})_{min}$ in the matrix. The same ranking holds for other compositions also.

Compatibility with Be-Rich Intermetallic Compounds

Whenever the Gibbs energies of formation data for Be-rich intermediate compounds were available, compatibility calculations were performed by procedures described in the section entitled "Theoretical Considerations." For a few of the Be-rich intermetallic compounds, although Gibbs free energies of formation data are not available, there are data on activity of Be in the compounds and these can be utilized to determine the compatibility of these compounds with NiAl alloys. The detailed procedures for these compounds are given in appendix E.

None of the Be-rich intermetallic compounds would be compatible with NiAl alloys because of the reduction of the beryllide with Ni component of the alloy matrix. Besides the beryllides given in table IX, there are several other Be-rich intermetallic compounds having high melting temperatures like $Be_{17}Hf_2$, $Be_{17}Nb_2$, $Be_{13}Th$, $Be_{12}Ti$. These compounds were not considered in our calculation due to the lack of adequate thermodynamic data for these compounds. However, based on the calculations for other Be-rich intermetallic compounds, it is more likely that these compounds would not be compatible with NiAl alloys.

Compatibility with Silicides

Based on the criteria that $(a_{Me})_{min}$ and $(a_{Si})_{min}$ must be less than 10^{-3} for a silicide to be compatible with NiAl alloys, none of the silicides appear to be compatible with NiAl alloys. However for two Mo-based silicides, Mo_3Si and Mo_5Si_3, it is determined that compatibility with alloys near the equiatomic composition would depend upon solubility of Mo in the matrix and, since the

solubility of Mo in NiAl alloys is negligible (ref. 10), it is likely that these two silicides might be compatible with NiAl alloys near the equiatomic composition.

List of Compatible Reinforcement Materials

Thermodynamic calculations have shown that there are several reinforcement materials that are likely to be compatible with NiAl alloys and a list of these is given below:

HfC, TiC, HfB_2, TiB_2, ScB_2, $Al2O_3$, BeO, Gd_2O_3, HfO_2, La_2O_3, Sc_2O_3, Y_2O_3, ZrO_2, $CaZrO_3$, and $Y_2O_3.2ZrO_2$; partially and fully stabilized ZrO_2, AlN, HfN, TiN, ZrN, Mo_3Si, Mo_5Si

Thermal Expansion Coefficients (CTE) for Reinforcement Materials

Besides chemical compatibility between the matrix and the reinforcement materials, the coefficient of thermal expansion for the fiber should match closely with that of the matrix. The CTE data for NiAl alloys are not available beyond 1100 K and therefore the coefficients of thermal expansion for compatible reinforcement materials will be compared with that of NiAl alloys at 1100 K only. The CTE for NiAl alloys at 1100 K is on the order of $16x10^{-6}$ K^{-1} (ref. 11). The thermal expansion coefficients for the compatible reinforcement materials at 1100 K in order of decreasing thermal expansion coefficients are given in table XV. The CTE data for all the compounds except for stabilized ZrO_2 were taken from the handbook on Thermal Expansion of Materials (refs. 11 and 12). The CTE data for 100 percent cubic ZrO_2 and partially stabilized ZrO_2 were taken from references 13 and 14, respectively. As can be seen from table XV, the thermal expansion coefficients for many of the compatible reinforcement materials are much lower than that of NiAl alloys. The CTE for a few oxides like La_2O_3, MgO, Cubic ZrO_2 (completely stabilized by CaO additions) are close to that of NiAl alloys. It is possible that suitable mixed oxide systems with reasonable thermal expansion coefficients and adequate mechanical properties could be developed for reinforcement in NiAl alloys.

SUMMARY OF RESULTS AND CONCLUSION

Chemical compatibility of several potential reinforcement materials with β' NiAl alloys with concentrations ranging from 40 to 50 at % Al have been analyzed from thermodynamic considerations. The reinforcement materials considered in this study include carbides, borides, oxides, nitrides, beryllides, and silicides. Among the carbides, TiC appears to be the only carbide that is compatible with all alloys within the concentration range 40 to 50 at % Al, although there are several other carbides like HfC and ZrC that would be compatible with alloys near the equiatomic composition. HfB_2, ScB_2, and TiB_2 appear to be the most promising candidates as reinforcement materials among all the borides. There are several oxides like Y_2O_3, Sc_2O_3, Gd_2O_3, La_2O_3, HfO_2, BeO, ZrO_2, and Al_2O_3 which would be compatible with all NiAl alloys within the concentration range 40 to 50 at % Al. There are several mixed oxides like $Al_2O_3 \cdot ZrO_2$, $CaZrO_3$, and $Y_2O_3 \cdot 2ZrO_2$ which are likely to be compatible with all NiAl alloys. Among nitrides, AlN, TiN, HfN, and ZrN appear to be promising.

None of the beryllides would be compatible with NiAl alloys. A few silicides like Mo_5Si_3 and Mo_3Si are also likely to be compatible with NiAl alloys.

There might be several other compatible reinforcement materials if the solubilities of the nonmetallic elements of the reinforcement materials like carbon and boron in the alloy matrix are very low. However, the reinforcement materials described in the previous paragraph appear to be the most promising ones.

Although there are several reinforcement materials which would be chemically compatible with NiAl alloys, there are only a few among these like La_2O_3, $CaZrO_3$, MgO, and cubic ZrO_2 whose coefficients of thermal expansion match closely with that of NiAl alloys. This severely restricts the choice of potential reinforcement materials and proper methods must be developed to alleviate the problem of thermal expansion mismatch between the matrix and the reinforcement material.

The reinforcement materials identified in this study are on the basis of thermodynamic considerations only; kinetic factors were not considered in this study. It is possible that there might be several reinforcement materials for which thermodynamics show that they would react with the matrix, but kinetics of the reactions might be very slow. In such cases the reinforcement materials would be acceptable if the reaction products do not adversely affect the performance of the composite system. Indeed, limited reaction between the reinforcement material and the matrix might be desirable for creating a strong bond between the two.

REFERENCES

1. Massalski, T.B., ed.: Binary Alloy Phase Diagrams, Vol. II, American Society of Metals, Metals Park, OH, 1986, p. 142.

2. Steiner, A.; and Komarek, K.L.: Thermodynamic Activities of Solid Nickel-Aluminum Alloys. Trans. Met. Soc. AIME, vol. 230, no. 4, June 1964, pp. 786-790.

3. Henig, E.T.; and Lukas, H.L.: Kalorimetrische Bestimmung der Bildungsenthalpie und die Beschreibung der Fehlordnung der Geordneten β-Phase $(Ni, Cu)_{1-x}Al_x$. Z. Metallkunde, vol. 66, no. 2, Feb. 1975, pp. 98-106.

4. Libowitz, G.G.: Point Defects and Thermodynamic Properties in CsCl-Type Intermetallic Compounds. Metall. Trans., vol. 2, no. 1, Jan. 1971, pp. 85-93.

5. Neumann, J.P.; Chang, Y.A.; and Lee, C.M.: Thermodynamics of Intermetallic Phases with the Triple-Defect B2 Structure. Acta Met., vol. 24, no. 7, July 1976, pp. 593-604.

6. Hanneman, R.E.; and Seybolt, A.U.: Nickel Activity Data in the Nickel-Aluminum System at 1000 °C. Trans. Met. Soc. AIME, vol. 245, no. 2, Feb. 1969, pp. 434-435.

7. Hultgren, R., et al.: Selected Values of the Thermodynamic Properties of Binary Alloys. American Society for Metals, Metals Park, OH, 1973.

8. Chase, M.W., Jr., et al.: JANAF Thermochemical Tables, 3rd ed., Parts I and II, J. Phys. Chem. Ref. Data, vol. 14, 1985, suppl. 1.

9. Barin, I.; and Knacke, O.: Thermochemical Properties of Inorganic Substances, Springer-Verlag, 1973.

10. Kaufman, L.; and Nesor, H.: Calculation of Superalloy Phase Diagrams: Part II. Metall. Trans., vol. 5, no. 7, July 1974, pp. 1623-1629.

11. Touloukian, Y.S., et al.: Thermophysical Properties of Matter, Vol. 12, IFI/Plenum, New York, 1975.

12. Touloukian, Y.S., et al.: Thermophysical Properties of Matter, Vol. 13, IFI/Plenum, New York, 1977.

13. Garvie, R.C.: Zirconium Dioxide and Some of its Binary Systems. High Temperature Oxides, Part II, A.M. Alper, ed., Academic Press, 1970, pp. 118-167.

14. Schubert, H.: Anisotropic Thermal Expansion Coefficients of Y_2O_3-Stabilized Tetragonal Zirconia. J. Am. Ceram. Soc., vol. 69, no. 3, Mar. 1986, pp. 270-271.

TABLE I. - REINFORCEMENT MATERIALS CONSIDERED IN THIS STUDY

Carbides	Borides	Oxides	Nitrides	Beryllides	Silicides
B_4C	AlB_{12}	Al_2O_3	AlN	$Be_{13}La$	Cr_3Si
HfC	CrB_2	BeO	BN	$Be_{13}Y$	Cr_5Si_3
Mo_2C	HfB_2	CaO	HfN	$Be_{13}Zr$	Mo_3Si
Nb_2C	LaB_6	CeO_2	LaN	$Be_{17}Nb_2$	Mo_5Si_3
NbC	NbB_2	Cr_2O_3	Si_3N_4	$Be_{17}Ti_2$	$MoSi_2$
SiC	ScB_2	Gd_2O_3	TaN		Nb_5Si_3
TaC	TaB_2	HfO_2	TiN		$NbSi_2$
Ta_2C	TiB_2	La_2O_3	ZrN		Ta_2Si
TiC	TiB	MgO			Ta_5Si_3
V_2C	VB	Sc_2O_3			$TaSi_2$
VC	VB_2	SiO_2			Ti_5Si_3
W_2C	V_3B_2	TiO			TiSi
WC	V_2B_3	TiO_2			V_3Si
ZrC	ZrB_2	Y_2O_3			V_5Si_3
		ZrO_2			VSi_2
		Ca_2SiO_4			W_5Si_3
		$CaZrO_3$			WSi_2
		$Y_2O_3 \cdot 2ZrO_2$			Zr_2Si
					Zr_5Si_3
					ZrSi

TABLE II. - ACTIVITIES OF Ni AND Al IN β' PHASE AT 1273 K

[Al activities are with respect to solid Al as reference state.]

Composition, at % Al	Activity of Al, a_{Al}	Activity of Ni, a_{Ni}
[a]36.3	3.72×10^{-5}	0.438
38	4.60×10^{-5}	.388
40	6.00×10^{-5}	.329
42	8.00×10^{-5}	.272
44	1.05×10^{-4}	.221
46	1.63×10^{-4}	.155
48	3.40×10^{-4}	.081
49	5.77×10^{-4}	.048
49.5	1.02×10^{-3}	.034
50	2.46×10^{-3}	.011
50.5	8.00×10^{-3}	3.1×10^{-3}
51	0.013	2.2×10^{-3}
52	.021	1.2×10^{-3}
54	.04	6.2×10^{-4}

[a]Phase boundary.

TABLE III. - ACTIVITIES OF Al AND Ni IN β' PHASE AT 1373 K

[Al activities are with respect to solid Al as reference state.]

Composition, at % Al	Activity of Al, a_{Al}	Activity of Ni, a_{Ni}
38	1.06×10^{-4}	0.419
40	1.38×10^{-4}	.355
42	1.84×10^{-4}	.294
44	2.42×10^{-4}	.238
46	3.76×10^{-4}	.167
48	7.84×10^{-4}	.087
49	1.33×10^{-3}	.051
49.5	2.35×10^{-3}	.036
50	4.16×10^{-3}	.016
50.5	9.97×10^{-3}	6.21×10^{-3}
51	0.016	4.41×10^{-3}
52	.026	2.54×10^{-3}
54	.026	1.23×10^{-3}

TABLE IV - ACTIVITIES OF Ni AND Al IN β' PHASE AT 1573 K

[Al activities are with repect to solid Al as reference state.]

Composition, at % Al	Activity of Al, a_{Al}	Activity of Ni, a_{Ni}
38	4.11×10^{-4}	0.476
40	5.36×10^{-4}	.403
42	7.15×10^{-4}	.333
44	9.38×10^{-4}	.271
46	1.45×10^{-3}	.19
48	3.04×10^{-3}	.099
49	5.15×10^{-3}	.058
49.5	9.11×10^{-3}	.041
50	9.81×10^{-3}	.03
50.5	0.014	8.53×10^{-3}
51	.022	3.49×10^{-3}
52	.037	2.70×10^{-3}
54	.071	1.71×10^{-3}

TABLE V. - COMPATIBILITY OF NiAl ALLOYS WITH CARBIDES

Reinforcement material	Temperature, K	Alloy composition, at % Al	Mode of reaction	Comments on compatibility
C	1373	40 - 50	Dissolution of C in the matrix	Depends upon solubility of C in the matrix
	1573	40 - 50	Dissolution of C in the matrix	Depends upon solubility of C in the matrix
B_4C	1373	<47	Ni_2B + free carbon formation	Not compatible
		48 - 50	Dissolution of B and C in the matrix; high values for both $(a_B)_{min}$ and $(a_C)_{min}$	Depends on the solubility of B and C in the matrix
	1573	<48	Ni_2B + free carbon formation	Not compatible
		49 - 50	Dissolution of B and C in the matrix; high values for both $(a_B)_{min}$ and $(a_C)_{min}$	Depends on the solubility of B and C in the matrix
HfC	1373	40 - 43	Dissolution of Hf and C in the matrix; high values for $(a_C)_{min}$	Depends on solubility of C in the matrix
		44 - 50	Dissolution of Hf and C in the matrix; low values for $(a_C)_{min}$ and $(a_{Hf})_{min}$	Compatible
	1573	40 - 45	Dissolution of Hf and C in the matrix; high values for $(a_C)_{min}$	Depends on solubility if C in the matrix
		46 - 50	Dissolution of Hf and C in the matrix; low values for $(a_C)_{min}$ and $(a_{Hf})_{min}$	Compatible
Mo_2C	1373 and 1573	40 - 50	Dissolution of Mo and C in the matrix; high values for both $(a_C)_{min.}$ and $(a_{Mo})_{min}$	Depends on solubility of Mo and C in the matrix
Nb_2C	1373	<43	NI_3Nb + free carbon formation	Not compatible
		44 - 48	Dissolution of Nb and C in in the matrix; high values for $(a_C)_{min}$	Depends on solubility of carbon in the matrix
		49 - 50	Dissolution of Nb and C in the matrix; low values for both $(a_C)_{min}$ and $(a_{Nb})_{min}$	Compatible
	1573	<43	Ni_3Nb + free carbon formation	Not compatible
		44 - 48	Dissolution of Nb and C in the matrix; high values for both $(a_{Nb})_{min}$ and $(a_C)_{min}$	Depends on solubility of Nb and C in the matrix
		49 - 50	Dissolution of Nb and C in in the matrix; high values for $(a_C)_{min}$	Depends on solubility of C in the matrix

TABLE V. - Continued.

Reinforcement material	Temperature, K	Alloy composition, at % Al	Mode of reaction	Comments on compatibility
NbC	1373 and 1573	40 - 46	Dissolution of Nb and C in in the matrix; high value for $(a_C)_{min}$	Depends on solubility of C in the matrix
		48 - 50	Dissolution of C and Nb in the matrix; low values for both $(a_C)_{min}$ and $(a_{Nb})_{min}$	Compatible
SiC	1373 and 1573	40 - 50	Ni_2Si + free carbon formation	Not compatible
TaC	1373	40 - 50	Dissolution of Ta and C in the matrix; low values for $(a_{Ta})_{min}$ and $(a_C)_{min}$	Compatible
	1573	40 - 44	Dissolution of Ta and C in th matrix; high values for $(a_C)_{min}$	Depends on solubility of C in the matrix
		46 - 50	Dissolution of C and Ta in the matrix; low values for $(a_C)_{min}$ and $(a_{Ta})_{min}$	Compatible
Ta_2C	1373	40 - 43	Dissolution of Ta and C in the matrix; high values for $(a_C)_{min}$	Depends on solubility of C in the matrix
		44 - 50	Dissolution of C and Ta in the matrix; low values for $(a_C)_{min}$ and $(a_{Ta})_{min}$	Compatible
	1573	40 - 44	Dissolution of Ta and C in the matrix; high values for $(a_C)_{min}$	Depends on solubility of C in the matrix
		46 - 50	Dissolution of C and Ta in the matrix; low values for $(a_C)_{min}$ and $(a_{Ta})_{min}$	Compatible
TiC	1373 and 1573	40 - 50	Dissolution of Ti and C in the matrix; low values for $(a_{Ti})_{min}$ and $(a_C)_{min}$	Compatible
V_2C	1373 and 1573	40 - 50	Dissolution of V and C in the matrix; high values for $(a_V)_{min}$	Depends on solubility of V in the matrix
VC	1373	40 - 50	Dissolution of V and C in the matrix; low values for $(a_V)_{min}$ and $(a_C)_{min}$	Compatible
	1573	40 - 50	Dissolution of V and C in the matrix; high values for $(a_V)_{min}$ and $(a_C)_{min}$	Depends on solubility of V and C in the matrix
W_2C	1373 and 1573	40 - 50	Dissolution of W and C in the matrix; high values for $(a_W)_{min}$	Depends on solubility of W in the matrix
WC	1373 and 1573	40 - 50	Dissolution of C and W in the matrix; high values for both $(a_C)_{min}$ and $(a_W)_{min}$	Depends on solubility of C and W in the matrix

TABLE V. - Concluded.

Reinforcement material	Temperature, K	Alloy composition, at % Al	Mode of reaction	Comments on compatibility
ZrC	1373 and 1573	40 - 46	Dissolution of Zr and C in the matrix; high values for $(a_C)_{min}$	Depends on solubility of C in the matrix
		48 - 50	Dissolution of C and Zr in the matrix; low values for $(a_C)_{min}$ and $(a_{Zr})_{min}$	Compatible

TABLE VI. - COMPATIBILITY OF NiAl ALLOYS WITH BORIDES

Reinforcement material	Temperature, K	Alloy composition, at % Al	Mode of reaction	Comments on compatibility
AlB_{12}	1373 and 1573	40 - 49	Ni_2B formed	Not compatible
		50	No reaction	Compatible
CrB_2	1373	40 - 46	Dissolution of Cr and B in the matrix; very high values for $(a_{Cr})_{min}$	Not compatible
		48 - 50	Dissolution of Cr and B in the matrix; high values for $(a_B)_{min}$	Depends on solubility of B in the matrix
	1573	40 - 50	Dissolution of Cr and B in the matrix; high values for $(a_{Cr})_{min}$ and $(a_B)_{min}$	Not compatible
HfB_2	1373 and 1573	40 - 50	Dissolution of Hf and B in the matrix; low values for $(a_{Hf})_{min}$ and $(a_B)_{min}$	Compatible
LaB_6	1373 and 1573	40 - 50	Dissolution of La and B in the matrix; low values for $(a_{La})_{min}$ and high values for $(a_B)_{min}$	Depends on solubility of B in the matrix
NbB_2	1373	40 - 43	Ni_3Nb + Ni_2B formation	Not compatible
		44 - 48	Dissolution of Nb and B in the matrix; high values for $(a_B)_{min}$	Depends on solubility of B in the matrix
		49 - 50	Dissolution of Nb and B in the matrix; low values for both $(a_{Nb})_{min}$ and $(a_B)_{min}$	Compatible
	1573	40 - 43	Ni_3Nb + Ni_2B formation	Not compatible
		44 - 50	Dissolution of Nb and B in the matrix; high values for $(a_B)_{min}$	Depends on solubility of B in the matrix
ScB_2	1373 and 1573	40 - 50	Dissolution of Sc and B in the matrix; low values for $(a_{Sc})_{min}$ and $(a_B)_{min}$	Compatible
TaB_2	1373 and 1573	40 - 50	Dissolution of Ta and B in the matrix; high values for $(a_B)_{min}$	Depends on solubility of B in the matrix
TiB_2	1373 and 1573	40 - 50	Dissolution of Ti and B in the matrix; low values for both $(a_{Ti})_{min}$ and $(a_B)_{min}$	Compatible

TABLE VI. - Continued.

Reinforcement material	Temperature, K	Alloy composition, at % Al	Mode of reaction	Comments on compatibility
TiB	1373	40 - 44	Dissolution of Ti and B in the matrirx; high values for $(a_B)_{min}$	Depends on solubility of B in the matrix
		46 - 50	Dissolution of Ti and B in the matrix; low values for both $(a_{Ti})_{min}$ and $(a_B)_{min}$	Commpatible
	1573	40 - 46	Dissolution of Ti and B in the matrix; high values for $(a_B)_{min}$	Depends on solubility of B in the matrix
		48 - 50	Dissolution of Ti and B in the matrix; low values for both $(a_{Ti})_{min}$ and $(a_B)_{min}$	Compatible
VB	1373	40 - 50	Dissolution of V and B in the matrix; low values for both $(a_V)_{min}$ and $(a_B)_{min}$	Compatbile
	1573	40 - 44	Dissolution of V and B in the matrix; high values for $(a_V)_{min}$	Depends on solubility of V in the matrix
		46 - 50	Dissolution of V and B in the matrix; low values for both $(a_V)_{min}$ and $(a_B)_{min}$	Compatible
VB_2	1373	40 - 50	Dissolution of V and B in the matrix; low values for both $(a_V)_{min}$ and $(a_B)_{min}$	Compatible
	1573	40 - 42	Dissolution of V and B in the matrix; high values for $(a_V)_{min}$	Depends on solubility of V in the matrix
		44 - 50	Dissolution of V and B in the matrix; low values for both $(a_V)_{min}$ and $(a_B)_{min}$	Compatible
V_3B_2	1373	40 - 44	Dissolution of V and B in the matrix; high values for $(a_V)_{min}$	Depends on solubility of V in the matrix
		46 - 50	Dissolution of V and B in the matrix; low values for both $(a_V)_{min}$ and $(a_B)_{min}$	Compatible
	1573	40 - 50	Dissolution of V and B in the matrix; high values for $(a_V)_{min}$	Depends on solubility of V in the matrix
V_2B_3	1373	40 - 50	Dissolution of V and B in the matrix; low values for both $(a_V)_{min}$ and $(a_B)_{min}$	Compatible
	1573	40 - 42	Dissolution of V and B in the matrix; high values for $(a_V)_{min}$	Depends on solubility of V in the matrix
		44 - 50	Dissolution of V and B in the matrix; low values for both $(a_V)_{min}$ and $(a_B)_{min}$	Compatible

TABLE VI. - Concluded.

Reinforcement material	Temperature, K	Alloy composition, at % Al	Mode of reaction	Comments on compatibility
ZrB_2	1373	~40	Dissolution of Zr and B in the matrix; high values for $(a_B)_{min}$	Depends on solubility of B in the matrix
		42 - 50	Dissolution of Zr and B in the matrix; low values for both $(a_{Zr})_{min}$ and $(a_B)_{min}$	Compatible
	1573	40 - 46	Dissolution of Zr and B in the matrix; high values for $(a_B)_{min}$	Depends on solubility of B in the matrix
		48 - 50	Dissolugion of Zr and B in the matrix; low values for both $(a_{Zr})_{min}$ and $(a_B)_{min}$	Compatible

TABLE VII. - COMPATIBILITY OF NiAl ALLOYS WITH OXIDES

Reinforcement material	Temperature, K	Alloy composition, at % Al	Mode of reaction	Comments on compatibility
Al_2O_3	1373 and 1573	40 - 50	No reaction	Compatible
BeO	1373 and 1573	40 - 50	Dissolution of Be in the matrix; low values for $(a_{Be})_{min}$	Compatible
CaO	1373 and 1573	40 - 49	Dissolution of Ca in the matrix; low values for $(a_{Ca})_{min}$	Compatible
		~50	Conditions might be just sufficient for formation of $CaAl_2O_4$ and $CaAl_2$	Borderline situation
CeO_2	1373 and 1573	40 - 46	Formation of Ni_5Ce and Al_2O_3	Not compatible
		47 - 49	Dissolution of Ce in the matrix; high values for $(a_{Ce})_{min}$	Depends on solubility of Ce in the matrix
		~50	Conditions might be just sufficient for formation of Al_2Ce and Al_2O_3	Not compatible
Cr_2O_3	1373 and 1573	40 - 50	Formation of Al_2O_3 and free Cr	Not compatible
Gd_2O_3	1373 and 1573	40 - 50	Dissolution of Gd in the matrix; low values for $(a_{Gd})_{min}$	Compatible
HfO_2	1373 and 1573	40 - 50	Dissolution of Hf in the matrix; low values for $(a_{Hf})_{min}$	Compatible
La_2O_3	1373 and 1573	40 - 50	Dissolution of La in the matrix; low values for $(a_{La})_{min}$	Compatible
MgO[a]	1373 and 1573	40 - 50	Formation of $MgAl_2O_4$ and Mg(g) for open system; P_{Mg} is on the order of 10^{-3} to 10^{-4} atm	Not compatible
MgO[b]	1373	40 - 48	Dissolution of Mg in the matrix; low values of $(a_{Mg})_{min}$	Compatible
		49 - 50	Dissolution of Mg in the matrix; high values for $(a_{Mg})_{min}$	Depends on solubility of Mg in the matrix
	1573	40	Dissolution of Mg in the matrix; low values for $(a_{Mg})_{min}$	Compatible
		42 - 50	Dissolution of Mg in the matrix; high values for $(a_{Mg})_{min}$	Depends on solubility of Mg in the matrix

[a]Open system.
[b]Closed system.

TABLE VII. - Concluded.

Reinforcement material	Temperature, K	Alloy composition, at % Al	Mode of reaction	Comments on compatibility
Sc_2O_3	1373 and 1573	40 - 50	Dissolution of Sc in the matrix; low values for $(a_{Sc})_{min}$	Compatible
SiO_2	1373 and 1573	40 - 50	Formation of Al_2O_3 and free Si	Not compatible
TiO	1373 and 1573	40 - 50	Dissolution of Ti in the matrix; high values for $(a_{Ti})_{min}$	Not compatible
TiO_2	1373 and 1573	40 - 50	Formation of Al_2O_3 and free Ti	Not compatible
Y_2O_3	1373 and 1573	40 - 50	Dissolution of Y in the matrix; low values for $(a_Y)_{min}$	Compatible
ZrO_2	1373 and 1573	40 - 42	Formation of Al_2O_3 and Ni_7Zr_2	Not compatible
		42 - 50	Dissolution of Zr in the matrix; low values for $(a_{Zr})_{min}$	Compatible
Ca_2SiO_4	1373 and 1573	40 - 50	Formation of Al_2O_3 and Ni_2Si	Not compatible

TABLE VIII. - COMPATIBILITY OF NiAl ALLOYS WITH NITRIDES

Reinforcement material	Temperature, K	Alloy composition, at % Al	Mode of reaction	Comments on compatibility
AlN	1373 and 1573	40 - 50	No reaction	Compatible
BN	1373 and 1573	40 - 50	Dissolution of B in the matrix; high values for $(a_B)_{min}$	Depends on solubility of B in the matrix
		~50	Conditions may be just sufficient for formation of AlN and AlB_{12}	May not be compatible
HfN	1373 and 1573	40 - 50	Dissolution of Hf in the matrix; low values for $(a_{Hf})_{min}$	Compatible
LaN	1373	~40	Dissolution of La in the matrix; low values for $(a_{La})_{min}$	Compatible
		42 - 50	Dissolution of La in the matrix; high values for $(a_{La})_{min}$	Depends on solubility of La in the matrix
	1573	40 - 50	Dissolution of La in the matrix; high values for $(a_{La})_{min}$	Depends on solubility of La in the matrix
Si_3N_4	1373 and 1573	40 - 50	Formation of AlN and free Si or formation of AlN and Ni_2Si	Not compatible
TaN	1373 and 1573	40 - 50	Dissolution of Ta in the matrix; high values for $(a_{Ta})_{min}$	Depends on solubility of Ta in the matrix
TiN	1373 and 1573	40 - 50	Dissolution of Ti in the matrix; low values for $(a_{Ti})_{min}$	Compatible
ZrN	1373 and 1573	40 - 50	Dissolution of Zr in the matrix; low values for $(a_{Zr})_{min}$	Compatible

TABLE IX. - COMPATIBILITY OF NiAl ALLOYS WITH Be-RICH INTERMETALLIC COMPOUNDS

Reinforcement material	Temperature, K	Alloy composition, at % Al	Mode of reaction	Comments on compatibility
$Be_{13}La$	1373 and 1573	40 - 50	Formation of NiBe and free La	Not compatible
$Be_{13}Y$	1373 and 1573	40 - 50	Formation of NiBe and free Y	Not compatible
$Be_{13}Zr$	1373 and 1573	40 - 50	Formation of NiBe and free Zr	Not compatible
$Be_{17}Nb_2$	1373 and 1573	40 - 50	Formation of NiBe and free Nb	Not compatible
$Be_{17}Ti_2$	1373 and 1573	40 - 50	Formation of NiBe and free Ti	Not compatible

TABLE X. - COMPATIBILITY OF NiAl ALLOYS WITH SILICIDES

Reinforcement material	Temperature, K	Alloy composition, at % Al	Mode of reaction	Comments on compatibility
Cr_3Si	1373 and 1573	40 - 45	Formation of Ni_2Si and free Cr	Not compatible
		46 - 50	Dissolution of Cr in the matrix; high values for $(a_{Cr})_{min}$	Not compatible
Cr_5Si_3	1373 and 1573	40 - 48	Formation of Ni_2Si and free Cr	Not compatible
		49 - 50	Dissolution of Cr in the matrix; very high values for $(a_{Cr})_{min}$	Not compatible
Mo_3Si	1373 and 1573	~40	Formation of Ni_2Si and free Mo	Not compatible
		42 - 50	Dissolution of Mo and Si in the matrix; high values for $(a_{Mo})_{min}$	Depends on solubility of Mo in the matrix
Mo_5Si_3	1373 and 1573	40 - 44	Formation of Ni_2Si and free Mo	Not compatible
		46 - 50	Dissolution of Mo and Si in the matrix; high values for $(a_{Mo})_{min}$	Depends on solubility of Mo in the matrix
$MoSi_2$	1373 and 1573	40 - 49	Formation of Ni_2Si and free Mo	Not compatible
		50	Dissolution of Mo and Si in the matrix; high values for $(a_{Mo})_{min}$	Depends on solubility of Mo in the matrix
Nb_5Si_3	1373 and 1573	40 - 48	Formation of Ni_2Si plus Ni-Nb compound (Ni_3Nb or Ni_6Nb_7)	Not compatible
		49 - 50	Dissolution of Nb and Si in the matrix; high values for $(a_{Nb})_{min}$	Depends on solubility of Nb in the matrix
$NbSi_2$	1373 and 1573	40 - 50	Formation of Ni_2Si plus Ni-Nb compound (Ni_3Nb or Ni_6Nb_7)	Not compatible
Ta_2Si	1373 and 1573	40 - 49.5	Formation of Ni_2Si and NiTa	Not compatible
		50	Dissolution of Ta and Si in the matrix; high values for both $(a_{Ta})_{min}$ and $(a_{Si})_{min}$	Depends on solubility of Ta and Si in the matrix

TABLE X. - Continued.

Reinforcement material	Temperature, K	Alloy composition, at % Al	Mode of reaction	Comments on compatibility
Ta_5Si_3	1373 and 1573	40 - 49.5	Formation of Ni_2Si and NiTa	Not compatible
		50	Dissolution of Ta and Si in the matrix; high values for both $(a_{Ta})_{min}$ and $(a_{Si})_{min}$	Depends on solubility of Ta and Si in the matrix
$TaSi_2$	1373 and 1573	40 - 50	Formation of Ni_2Si and NiTa	Not compatible
Ti_5Si_3	1373	40 - 44	Formation of Ni_2Si and Ni_3Ti	Not compatible
		46 - 49	Dissolution of Ti and Si in the matrix; high values for $(a_{Ti})_{min}$	Not compatible
		50	Dissolution of Ti and Si in the matrix; low values for both $(a_{Ti})_{min}$ and $(a_{Si})_{min}$	Compatible
	1573	40 - 44	Formation of Ni_2Si and Ni_3Ti	Not compatible
		46 - 50	Dissolution of Ti and Si in the matrix; high values for $(a_{Ti})_{min}$	Not compatible
TiSi	1373 and 1573	40 - 46	Formation of Ni_2Si and Ni-Ti compound (NiTi or Ni_3Ti)	Not compatible
		48 - 50	Dissolution of Ti and Si in the matrix; high values for $(a_{Ti})_{min}$	Not compatible
V_3Si	1373 and 1573	40 - 50	Dissolution of V and Si in the matrix; high values for $(a_V)_{min}$	Depends on solubility of V in the matrix
V_5Si_3	1373 and 1573	40 - 50	Dissolution of V and Si in the matrix; high values for $(a_V)_{min}$	Depends on solubility of V in the matrix
VSi_2	1373 and 1573	40 - 49	Formation of Ni_2Si and free V	Not compatible
		50	Dissolution of V and Si in the matrix; high values for $(a_V)_{min}$	Depends on solubility of V in the matrix
W_5Si_3	1373 and 1573	40 - 50	Formation of Ni_2Si plus free W	Not compatible
WSi_2	1373 and 1573	40 - 50	Formation of Ni_2Si plus free W	Not compatible

TABLE X. - Concluded.

Reinforcement material	Temperature, K	Alloy composition at % Al	Mode of reaction	Comments on compatibility
Zr_2Si	1373 and 1573	40 - 47	Formation of Ni_7Zr_2 and free Si	Not compatible
		47 - 49	Formation of Ni_2Si and Ni-Zr compound; (NiZr or Ni_7Zr_2)	Not compatible
		50	Dissolution of Zr and Si in the matrix; high values for $(a_{Zr})_{min}$	Depends on solubility of Zr in the matrix
Zr_5Si_3	1373 and 1573	40 - 46	Formation of Ni_7Zr_2 and free Si	Not compatible
		46 - 49	Formation of Ni_2Si and Ni-Zr compound; (Ni_7Zr_2 or NiZr)	Not compatible
	1373	50	Dissolution of Zr and Si in the matrix; low values for both $(a_{Zr})_{min}$ and $(a_{Si})_{min}$	Compatible
	1573	50	Dissolution of Zr and Si in the matrix; high values for $(a_{Zr})_{min}$	Depends on solubility of Zr in the matrix
ZrSi	1373 and 1573	40 - 48	Formation of Ni_2Si and Ni-Zr compound; (Ni_7Zr_2 and NiZr)	Not compatible
		49 - 50	Dissolution of Zr and Si in the matrix; low values for both $(a_{Si})_{min}$ and $(a_{Zr})_{min}$	Compatible

TABLE XI. - CARBIDES IN ORDER OF DECREASING $(a_{Me})_{min}$ AND $(a_C)_{min}$ IN Ni-50Al

[T = 1573 K]

Carbide	$(a_{Me})_{min}$	Carbide	$(a_C)_{min}$
HfC	5.4×10^{-8}	HfC	3.4×10^{-6}
ZrC	9.1×10^{-7}	TiC	4.1×10^{-6}
TiC	3.2×10^{-6}	Ta_2C	1.4×10^{-5}
TaC	2.3×10^{-5}	ZrC	5.7×10^{-5}
NbC	2.9×10^{-5}	NbC	1.4×10^{-4}
Ta_2C	5.1×10^{-4}	TaC	1.6×10^{-4}

TABLE XII. - BORIDES IN ORDER OF DECREASING $(a_{Me})_{min}$ AND $(a_B)_{min}$ IN Ni-50Al [T = 1573 K]

Boride	$(a_{Me})_{min}$	Boride	$(a_B)_{min}$
HfB_2	1.97×10^{-10}	ScB_2	7.99×10^{-6}
ScB_2	4.3×10^{-10}	HfB_2	1.15×10^{-5}
ZrB_2	1.26×10^{-9}	TiB_2	7.52×10^{-5}
TiB_2	2.82×10^{-8}	VB	4.81×10^{-5}
VB2	4.12×10^{-6}	TiB	8.94×10^{-5}
V_2B_3	2.02×10^{-5}	ZrB_2	1.12×10^{-4}
VB	1.25×10^{-4}	V_2B_3	2.89×10^{-4}
TiB	1.82×10^{-4}	VB_2	7.82×10^{-4}

TABLE XIII. - OXIDES IN ORDER OF DECREASING $(a_{Me})_{min}$ IN Ni-50Al [T = 1573 K]

Oxide	$(a_{Me})_{min}$
Y_2O_3	2.92×10^{-7}
Sc_2O_3	4.34×10^{-7}
Gd_2O_3	8.44×10^{-6}
La_2O_3	1.27×10^{-5}
HfO_2	8.42×10^{-5}
BeO	4.24×10^{-4}
ZrO_2	7.41×10^{-4}

TABLE XIV. - NITRIDES IN ORDER OF DECREASING $(a_{Me})_{min}$ IN Ni-50Al MATRIX [T = 1573 K]

Nitride	$(a_{Me})_{min}$
HfN	1.54×10^{-5}
ZrN	5.12×10^{-5}
TiN	4.37×10^{-4}

TABLE XV. - COEFFICIENT OF THERMAL EXPANSION FOR COMPATIBLE REINFORCEMENT MATERIALS

Reinforcement material	Coefficient of thermal expansion at 1100 K, K^{-1}
La_2O_3	15.3×10^{-6}
MgO	15.2
ZrO_2[a]	~13
$CaZrO_3$	12.5
ZrO_2[b]	10.6
BeO	10.6
Sc_2O_3	10.2
TiN	10.1
Gd_2O_3	9.5
Al_2O_3	9.4
HfO_2	8.9
Y_2O_3	8.8
TiB_2	8.5
ZrN	8.5
TiC	8.3
HfB_2	7.5
ZrO_2[c]	7.5
Mo_3Si	7.5
HfC	7.1
AlN	6.2

[a] ZrO_2, 100 percent cubic, fully stabilized by CaO additions.
[b] ZrO_2 containing 3 mole percent Y_2O_3, partially stabilized tetragonal ZrO_2.
[c] Pure ZrO_2.

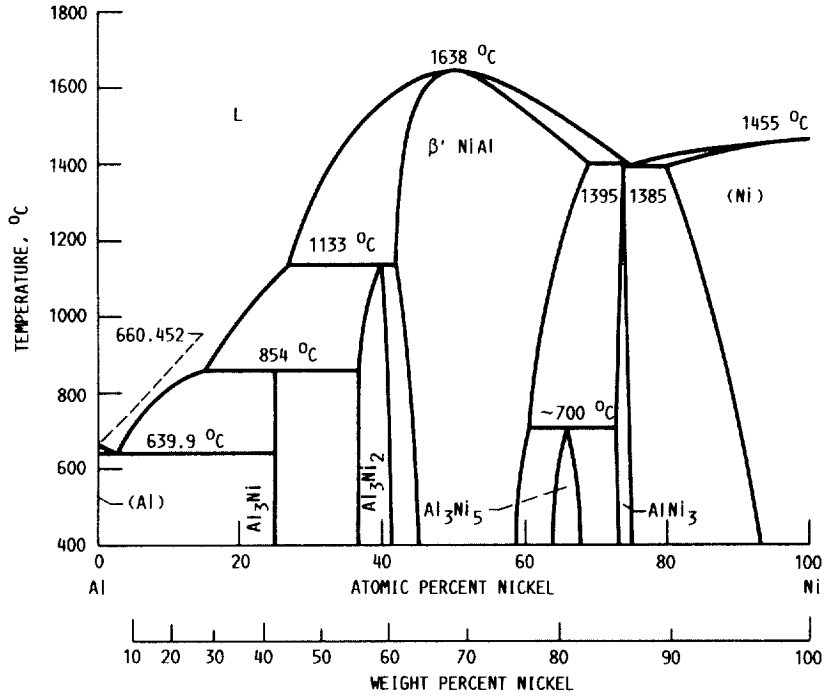

FIGURE 1. - Ni-Al PHASE DIAGRAM (REF. 1).

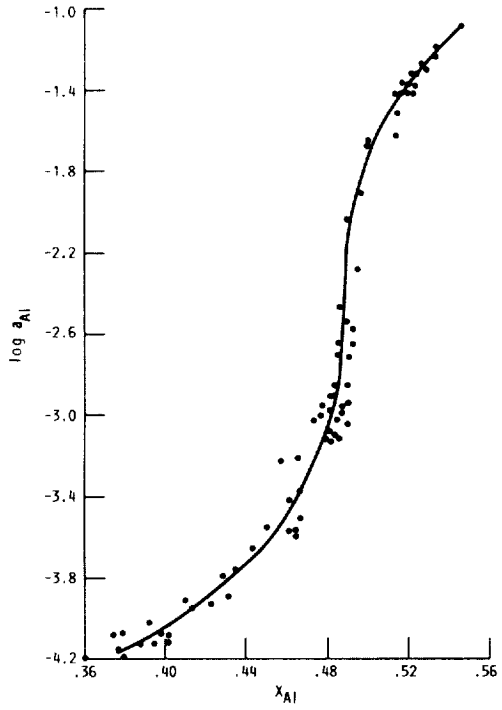

FIGURE 2. - Al ACTIVITY DATA OF KOMAREK AND STEINER (REF. 2) AT 1273 K.

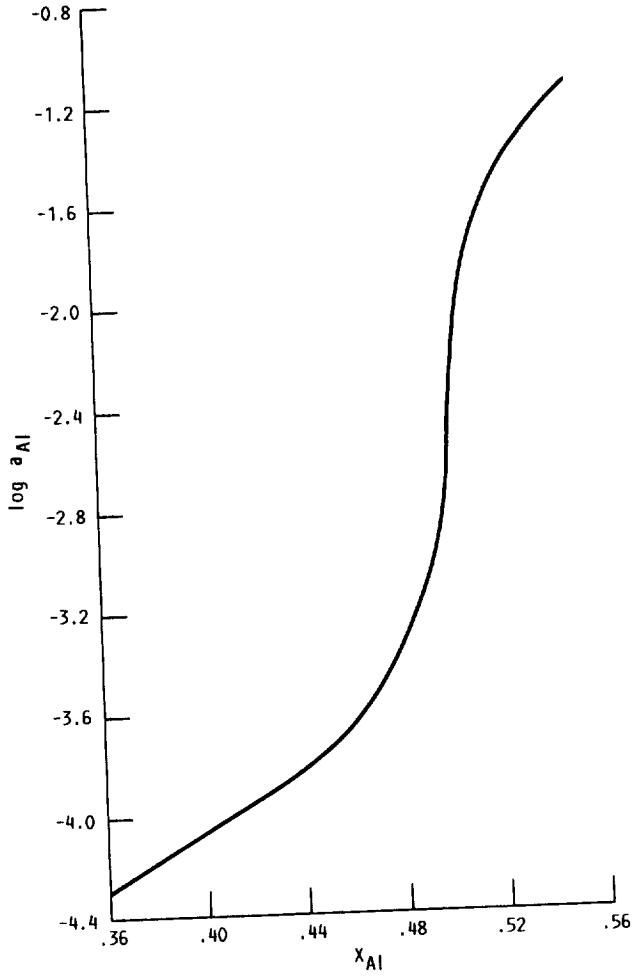

FIGURE 3. - REVISED AND SMOOTHED ACTIVITY DATA FOR Al IN β′ Ni-Al PHASE AT 1273 K.

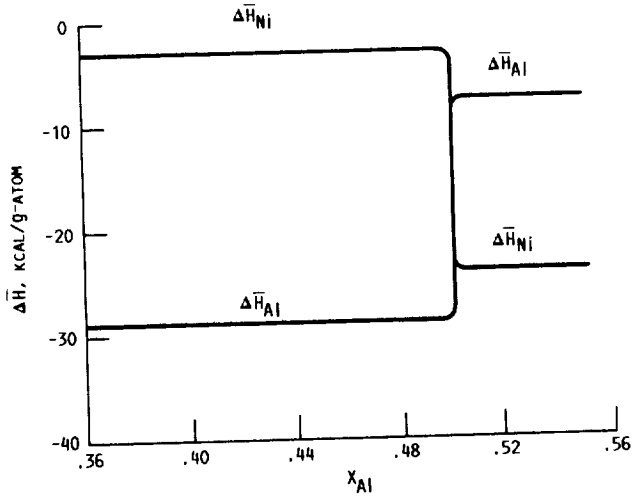

FIGURE 4. - PARTIAL MOLAR ENTHALPIES OF Ni AND Al AS A FUNCTION OF Al CONCENTRATION IN THE ALLOY. (DATA OF HENIG AND LUKAS, REF. 3).

APPENDIX A
GIBBS ENERGIES OF FORMATION OF COMPOUNDS AT 1373 AND 1573 K

Compound	$-\Delta G_f^\circ$ at 1373 K, kCal/mol	$-\Delta G_f^\circ$ at 1573 K, kCal/mol	Comments on thermodynamic data
Al_2Zr	40.8	40.8	ΔG_f° same as that at 1023 K, obtained from compilations by Hultgreen and Desai (ref. 1)
Al_3Zr_2	64.0	64.0	
Al_3Zr_4	72.1	72.1	
Al_3V	4.1	4.1	
Al_8V_5	19.6	19.6	
Al_4W	12.2	12.1	From Kaufman and Nesor (ref. 2)
Al_2Hf	40.8	40.8	Estimated to be the same as Al_2Zr
AlB_{12}	50.5	50.2	
Al_4C_3	36.4	33.1	
AlN	41.2	35.9	
Al_2O_3	297.9	282.9	
BN	31.2	27.1	
B_4C	13.8	13.4	
BeO	113.4	108.9	
$Be_{13}Y$	54.2	54.2	ΔG_f° same as that at 1330 K, obtained from Hultgreen and Desai (ref. 1)
$Be_{13}Zr$	56.4	56.4	
$CaAl_2(l)$	46.6	47.2	
CaO	117.9	113.0	
Ca_2SiO_4	413.6	396.0	
$CaZrO_3$	327.5	313.9	
$CeAl_2$	38.3	37.0	
CeO_2	193.2	183.5	
CrB_2	25.7	25.4	
Cr_2O_3	184.1	172.0	
Cr_3Si	24.4	24.3	
Cr_5Si_3	57.8	58.6	
Cr_4Al_6	60.2	61.0	From Kaufman and Nesor (ref. 2)
Gd_2O_3	340.3	327.0	
HfB_2	76.4	75.8	
HfC	52.6	52.2	
HfN	60.0	56.0	
HfO_2	206.7	198.6	
$LaAl_2$	29.0	27.1	
LaB_6	95.6	95.6	ΔG_f° same as ΔH_{298}°, obtained from Topor and Kleppa (ref. 3)
LaN	36.5	31.3	
La_2O_3	335.9	322.7	

Compound	$-\Delta G_f^\circ$ at 1373 K, kCal/mol	$-\Delta G_f^\circ$ at 1573 K, kCal/mol	Comments on thermodynamic data
MgO	108.6	103.5	With respect to solid Mg as the standard reference state
MgO	107.7	97.8	With respect to gaseous Mg as the standard reference state
Mo_3Al	17.0	17.8	From Kaufman and Nesor (ref. 2)
MoAl	8.0	9.4	From Kaufman and Nesor (ref. 2)
Mo_2Al_3	20.4	24.0	From Kaufman and Nesor (ref. 2)
Mo_3Al_8	51.9	55.9	From Kaufman and Nesor (ref. 2)
Mo_2C	12.6	12.8	
Mo_3Si	28.0	27.9	
Mo_5Si_3	76.5	76.7	
$MoSi_2$	30.9	30.7	
Nb_3Al	29.2	27.4	
Nb_2Al	26.2	24.6	From Kaufman and Nesor (ref. 2)
$NbAl_3$	41.6	38.2	
NbB_2	38.7	38.3	
NbC	32.7	32.7	
Nb_2C	42.5	41.9	
Nb_5Si_3	112.1	112.7	
$NbSi_2$	31.1	30.7	
Ni_2B	15.9	18.9	Estimated in this study (See Appendix C)
NiBe	19.6	19.6	ΔG_f° same as that of 1100 K, from compilations by Hultgreen and Desai (ref. 1)
$NiBe_4$	35.3	35.3	
Ni_5Ce	47.6	47.6	ΔG_f° same as ΔH_{298}°, from Colinet and Pasturel (ref. 4)
Ni_3Gd	35.9	Not stable	ΔG_f° same as ΔH_{298}°, from Colinet et al. (ref. 5)
Ni_7Gd_2	76.1	Not stable	
Ni_5Gd	44.9	44.9	
Ni_5Hf	48.3	48.3	Assumed to be same as for Ni_5Zr
Ni_7Hf_2	91.8	91.8	Assumed to be same as for Ni_7Zr_2
$Ni_{10}Hf_7$	203.5	203.5	Assumed to be same as for $Ni_{10}Zr_7$

Compound	$-\Delta G_f^\circ$ at 1373 K, kCal/mol	$-\Delta G_f^\circ$ at 1573 K, kCal/mol	Comments on thermodynamic data
NiHf	23.9	23.9	Assumed to be same as for NiZr
$NiHf_2$	26.5	26.5	Assumed to be same as for $NiHf_2$
Ni_5La	32.2	31.8	Extrapolated from Rezukhina and Kutsev's data (ref. 6)
NiMo	0.5	0.6	From Kaufman and Nesor (ref. 7)
Ni_3Nb	32.2	32.2	From Kaufman and Nesor (ref. 7)
Ni_6Nb_7	109.3	Not stable	From Kaufman and Nesor (ref. 7)
Ni_2Si	34.1	34.1	ΔG_f° same as that 1583 K, estimated in this study (see appendix B)
NiTa	17.8	17.8	ΔG_f° same as ΔH_{298}°, obtained from Watson and Bennett (ref. 8)
NiTi	12.5	11.7	
Ni_3Ti	26.1	24.6	
Ni_4W	5.4	5.6	From Kaufman and Nesor (ref. 7)
$Ni_{17}Y_2$	54.0	53.2	Extrapolated from Subramanian and Smith's data (ref. 9)
Ni_5Y	27.6	27.2	
Ni_4Y	27.5	27.1	
Ni_7Y_2	55.2	54.5	
Ni_3Y	25.5	Not stable	
Ni_5Zr	48.3	48.3	ΔG_f° same as ΔH_{298}°, ΔH_{298}° taken to be the average of two sets of data: One set from Henaff et al. (ref. 10) and the other set from Gachon and Hertz (ref. 11)
Ni_7Zr_2	91.8	91.8	
$Ni_{10}Zr_7$	203.5	203.5	
NiZr	23.9	23.9	
$NiZr_2$	26.5	26.5	
ScB_2	73.4	73.4	ΔG_f° same as ΔH_{298}°, taken from Topor and Kleppa (ref. 12)
Sc_2O_3	359.1	345.4	
SiC	13.4	12.9	
SiO_2	159.1	150.9	
Si_3N_4	69.4	53.9	
TaB_2	46.9	46.4	
TaC	33.6	33.7	
Ta_2C	47.5	47.4	
TaN	31.6	27.9	

Compound	$-\Delta G_f^\circ$ at 1373 K, kCal/mol	$-\Delta G_f^\circ$ at 1573 K, kCal/mol	Comments on thermodynamic data
Ta_2N	33.2	29.2	
Ta_5Si_3	84.4	85.1	
Ta_2Si	31.1	31.3	
$TaSi_2$	21.1	20.0	
TiAl	14.5	14.3	
Ti_3Al	14.7	13.1	
TiB	32.3	29.9	
TiB_2	61.1	60.0	
TiC	40.2	39.5	
TiN	49.8	45.4	
TiO	98.8	94.7	
TiO_2	166.1	157.5	
Ti_5Si_3	140.9	140.8	
TiSi	30.8	30.7	
$TiSi_2$	29.9	29.6	
VB	31.3	31.1	
VB_2	45.2	44.7	
V_3B_2	69.0	68.4	
V_2B_3	77.3	76.5	
V_2C	34.3	34.2	
VC	21.5	21.0	
VN	24.3	20.5	
V_3Si	33.9	33.3	
V_5Si_3	123.5	128.0	
VSi_2	34.5	35.1	
W_2C	20.1	22.3	
WC	8.3	8.2	
W_5Si_3	41.1	42.5	
WSi_2	19.8	19.4	
Y_2O_3	361.1	347.9	
$Y_2O_3 \cdot 2ZrO_2$	767.1	736.4	
ZrB_2	71.1	69.8	
ZrC	44.0	43.5	
ZrN	56.5	52.1	
ZrO_2	200.4	191.7	
Zr_2Si	49.6	49.1	
Zr_5Si_3	137.5	136.3	
ZrSi	36.2	35.8	
$ZrSi_2$	35.1	34.4	

REFERENCES FOR APPENDIX A

1. Hultgren, R., et al.: Selected Values of Thermodynamic Properties of Binary Alloys. American Society of Metals, Metals Park, OH, 1973.

2. Kaufman, L.; and Nesor, H.: Coupled Phase Diagrams and Thermochemical Data for Transition Metal Binary Systems - 5. CALPHAD, vol. 2, no. 4, 1978, pp. 325-348.

3. Topor, L.; and Kleppa, O.J.: Standard Molar Enthalpy of Formation of LaB_6 by High-Temperature Calorimetry. J. Chem. Thermodynamics, vol. 16, no. 10, Oct. 1984, pp. 993-1002.

4. Colinet, C.; and Pasturel, A.: A Thermodynamic Study of Cerium Behaviour in Hexagonal $CeNi_5$ Compound. Phys. Stat. Sol. (a), vol. 80, 1983, pp. K75-K79.

5. Colinet, C.; Pasturel, A.; and Buschow, K.H.J.: Study of the Enthalpies of Formation in the Gd-Ni System. Metall. Trans. A, vol. 17, no. 5, May 1986, pp. 777-780.

6. Rezukhina, T.N.; and Kutsev, S.V.: Thermodynamic Properties of Intermetallic Compounds in the La-Ni System. Russ. J. Phys. Chem. (Engl. Transl.), vol. 56, no. 1, Jan. 1982, pp. 1-6.

7. Kaufman, L.; and Nesor, H.: Coupled Phase Diagrams and Thermochemical Data for Transition Metal Binary Systems - 2. CALPHAD, vol. 2, no. 1, 1978, pp. 81-108.

8. Watson, R.E.; and Bennett, L.H.: Optimized Prediction for Heats of Formation of Transition Metal Alloys. CALPHAD, vol. 5, no. 1, 1981, pp. 25-40.

9. Subramanian, P.R.; and Smith, J.F.: Thermodynamics of Formation of Y-Ni Alloys. Metall. Trans. B., vol. 16, no. 3, Sept. 1985, pp. 577-584.

10. Henaff, M.P., et al.: Study of the Enthalpies of Formation and Crystallization in the System Zr-Ni. J. Appl. Phys., vol. 56, no. 2, July 15, 1984, pp. 307-310.

11. Gachon, J.C.; and Hertz, J.: Enthalpies of Formation of Binary Phases in the Systems FeTi, FeZr, CoTi, CoZr, NiTi, and NiZr, by Direct Reaction Calorimetry. CALPHAD, vol. 7, no. 1, 1983, pp. 1-12.

12. Topor, L.; and Kleppa, O.J.: Enthalpies of Formation of First-Row Transition-Metal Diborides by a New Calorimetric Method. J. Chem. Thermodynamics, vol. 17, no. 11, Nov. 1985, pp. 1003-1016.

APPENDIX B
ESTIMATION OF GIBBS ENERGY OF FORMATION OF Ni_2Si

From the NiSi phase diagram (ref. 1) the melting point of Ni_2Si is 1583 K. At the melting point the Gibbs free energy for solid Ni_2Si would be the same as that for liquid of the same composition. Thus, if thermodynamic data for the liquid at the melting point are available, the Gibbs energy of formation for Ni_2Si can be calculated from such data.

Schwerdtfeger and Engell (ref. 2) have measured the activities of Si in NiSi melts in the temperature range 1753 to 1883 K and have derived the activities for Ni by Gibbs-Duhem integration. From Si and Ni activity data the excess Gibbs energy of mixing in the melt can be calculated from the expression

$$G^{xs} = RT(X_{Si} \times \ln \gamma_{Si} + X_{Ni} \times \ln \gamma_{Ni}) \qquad (1B)$$

where G^{xs} is the excess Gibbs energy of mixing in the melt; X_{Si} and X_{Ni} are the mole fractions of Si and Ni in the melt, respectively; γ_{Si} and γ_{Ni} are the activity coefficients of Si and Ni in the melt, respectively. Figure B1 shows a linear relationship between G^{xs} and temperature for a melt corresponding to the Ni_2Si composition (X_{Si} = 0.333 and X_{Ni}= 0.666) and extrapolation of this curve gives G^{xs} at 1583 K to be -9.85 kCal/g-atom for $Ni_2Si(l)$. The Gibbs energy of mixing in the melt (G^M) at any temperature can be calculated from the expression:

$$G^M = RT(X_{Si} \times \ln X_{Si} + XNi \times \ln X_{Ni}) + RT(X_{Si} \times \ln \gamma_{Si} + X_{Ni} \times \ln \gamma_{Ni}) \qquad (2B)$$

G^M for a melt corresponding to the Ni_2Si composition is calculated to be -11.85 kCal/g-atom. The Gibbs energy of formation of Ni_2Si from solid Ni and Si can be calculated by adding the ΔG values for the following reactions:

$$0.666Ni(l) + 0.333Si(l) = Ni_{0.666}Si_{0.333}(l) \qquad (3B)$$

$$0.666Ni(s) = 0.666Ni(l) \qquad (4B)$$

$$0.333Si(s) = 0.333Si(l) \qquad (5B)$$

$$Ni_{0.666}Si_{0.333}(l) = Ni_{0.666}Si_{0.333}(s) \qquad (6B)$$

ΔG for the reaction in eq. (3B) is the Gibbs energy of mixing in the melt (-11.85 kCal); ΔG for the reaction in eq. (4B) is the Gibbs energy of fusion of Ni at 1583 K which is obtained to be 0.223 kCal; ΔG for the reaction in eq. (5B) is the Gibbs energy of fusion for Si at 1583 K and obtained to be 0.32 kCal; ΔG for the reaction in eq. (6B) is zero at the melting point of Ni_2Si. Thus the Gibbs energy change for the reaction

$$0.666Ni(s) + 0.333Si(s) = Ni_{0.666}Si_{0.333}(s) \qquad (6B)$$

is calculated to be -11.376 kCal and correspondingly the Gibbs energy of formation of Ni_2Si from solid Ni and Si is calculated to be -34.13 kCal/mole at 1583 K.

ESTIMATION OF GIBBS ENERGIES OF FORMATION OF Ni_2B AND Ni_3B

In the Ni-B system two compounds, Ni_2B and Ni_3B, have melting points greater than 1373 K and therefore, only these two compounds will be considered in the present study. The melting points of Ni_2B and Ni_3B are 1400 and 1425 K, respectively (ref. 1). Storms and Szklarz (ref. 3) have measured the activity of nickel as a function of composition in the temperature range 1400 to 1800 K. Activity of B in the melt can be calculated via Gibbs-Duhem integration. Activities obtained from Storms and Szklarz's paper are with reference to solid Ni and B as the standard reference state and therefore Gibbs energy of mixing in the melt with reference to solid Ni and B at the melting temperatures for the compounds would be the same as the Gibbs energy of formation of these solid compounds. Thus the Gibbs energy of formation of a given Ni-B compound can be computed from the expression:

$$\Delta G_f^\circ = G^M = RT(X_{Ni} \times \ln a_{Ni} + X_B \times \ln a_B) \qquad (7B)$$

From Storms and Szklarz's data activities of Ni and B in a melt corresponding to Ni_3B composition and at the melting point of Ni_3B are 0.55 and 8.22×10^{-3}, respectively. Using these activity values in eq. (7B), the Gibbs energy of formation of Ni_3B at 1425 K is calculated to be -18.66 kCal/mol. The activities of Ni and B in the melt corresponding to Ni_2B composition and at the melting point of this compound (1398 K) are 0.24 and 5.68×10^{-2}, respectively and, using these values in eq. (7B), the Gibbs energy of formation of Ni_2B at 1398 K is calculated to be -15.92 kCal/mol. From the activity data at 1573 K, the Gibbs energy of formation of $Ni_2B(l)$ at 1573 K from solid Ni and B is estimated to be -18.89 kCal/mol.

REFERENCES FOR APPENDIX B

1. T. B. Massalski, Binary Alloy Phase Diagrams, American Society of Metals, Metals Park, OH (1986).

2. K. Schwerdtfeger and H. J. Engell, "Activity Measurements In Nickel-Silicon Melts in the Temperature Range 1480° to 1610 °C", Trans. Met. Soc. AIME, Vol. 233, pp 1327-1332 (1965).

3. E. K. Storms and E. G. Szklarz, "Vaporization Thermodynamics of Ni-B (liquid) and Ni-B-C (liquid)", J. Less Common Metals, Vol. 135, pp 229 - 237 (1987).

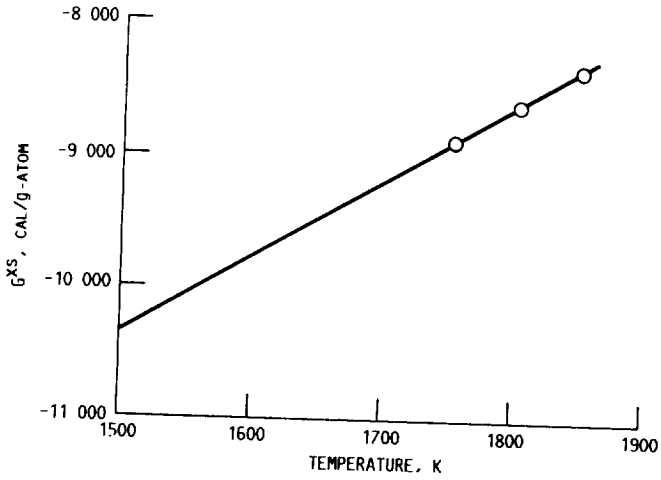

FIGURE B1. - G^{XS} AS A FUNCTION OF TEMPERATURE FOR A Ni-Si MELT OF COMPOSITION Ni-33 at % Si.

APPENDIX C
POSSIBLE STABLE PRODUCT COMPOUNDS IN THE MATRIX

The stable product compounds that can possibly be formed in the matrix as a result of interaction of the NiAl alloys with different elements of the reinforcement material are given in the following table:

Element	Temperature, K,	Alloy composition at % Al	Stable compound
B	1373 and 1573	>49	AlB_{12}
		<49	Ni_2B
Be	1373 and 1573	40 - 50	NiBe
C	1373	>53	Al_4C_3
		<53	No stable compound
	1573	>54	Al_4C_3
		<54	No stable compound
Ca	1373 and 1573	>44	Al_2Ca(l)
		<44	$Ni_{0.6}Ca_{0.4}$(l)
Ce	1373	>49.5	Al_2Ce
		<49.5	Ni_5Ce
	1573	>49	Al_2Ce
		<49	Al_2Ce
Cr	1373 and 1573	40 - 50	No stable compound
Gd	1373	>46	Ni_3Gd
		<45	Ni_5Gd
	1573	>49	No stable compound
		<49	Ni_5Gd

Element	Temperature, K,	Alloy composition, at % Al	Stable compound
Hf	1373	>49.5	Al_2Hf
		<49.5	Ni_7Hf_2
	1573	>50.5	Al_2Hf
		49 - 50	NiHf
		<48	Ni_7Hf_2
La	1373 and 1573	>49	Al_2La
		<49	Ni_5La
Mo	1373 and 1573	>50	Mo_3Al
		<50	No stable compound
N	1373 and 1573	40 - 50	AlN
Nb	1373	>50.5	Nb_2Al
		49 - 50	Ni_6Nb_7
		<48	Ni_3Nb
	1573	>50	Nb_2Al
		<49.5	Ni_3Nb
O	1373 and 1573	40 - 50	Al_2O_3
Sc	(a)	(a)	(a)
Si	1373 and 1573	<52	Ni_2Si

[a]No thermodynamic data for NiSc compounds.

Element	Temperature, K,	Alloy composition, at % Al	Stable compound
Ta	1373 and 1573	<52	NiTa
Ti	1373	>50.5	AlTi
		49 - 50	NiTi
		<49	Ni_3Ti
	1573	>50.5	AlTi
		48 - 50	NiTi
		<48	Ni_3Ti
V	1373 and 1573	40 - 50	No stable compound
W	1373 and 1573	40 - 50	No stable compound
Y	1373	50	No stable compound
		48 - 49	Ni_3Y
		<48	Ni_7Y_2
	1573	49 - 50	No stable compound
		<48	Ni_7Y_2
Zr	1373	>50	Al_2Zr
		<50	Ni_7Zr_2
	1573	>50.5	Al_2Zr
		49 - 50	NiZr
		<49	Ni_7Zr_2

APPENDIX D
MINIMUM ACTIVITIES OF ELEMENTS OF REINFORCEMENT MATERIAL IN THE MATRIX

This appendix gives the minimum calculated values for the elements of the reinforcement material in the matrix as a function of alloy composition for different reinforcement materials. The activities will be given only for those reinforcement materials for which thermodynamic calculations have shown that dissolution of the elements of the reinforcement material in the matrix is the predominant mode of reaction.

B_4C

Alloy composition, at %	$(a_B)_{min}$, 1373 K	$(a_C)_{min}$, 1373 K	$(a_B)_{min}$, 1573 K	$(a_C)_{min}$, 1573 K
50	0.28	0.49	0.34	0.62
49	.28	.33	.34	.5

HfC

Alloy composition, at %	$(a_{Hf})_{min}$, 1373 K	$(a_C)_{min}$, 1373 K	$(a_{Hf})_{min}$, 1573 K	$(a_C)_{min}$, 1573 K
50	4.16×10^{-9}	4.24×10^{-7}	5.41×10^{-8}	3.39×10^{-6}
48	↓	1.64×10^{-5}	↓	3.86×10^{-5}
46		1.60×10^{-4}		3.78×10^{-4}
44		5.55×10^{-4}		1.31×10^{-3}
40		2.23×10^{-3}		5.25×10^{-3}

Mo_2C

Alloy composition, at %	$(a_{Mo})_{min}$, 1373 K	$(a_C)_{min}$, 1373 K	$(a_{Mo})_{min}$, 1573 K	$(a_C)_{min}$, 1573 K
50	0.098	0.04	0.127	0.066
$\leq$49	.098	9.79×10^{-3}	.127	.016

Nb_2C

Alloy composition, at %	$(a_{Nb})_{min}$, 1373 K	$(a_C)_{min}$, 1373 K	$(a_{Nb})_{min}$, 1573 K	$(a_C)_{min}$, 1573 K
50	4.17×10^{-4}	1.08×10^{-5}	1.22×10^{-3}	3.81×10^{-5}
49	↓	5.68×10^{-5}	↓	5.22×10^{-5}
48		1.40×10^{-3}		1.29×10^{-3}
46		0.07		0.064
44		.58		.54

NbC

Alloy composition, at %	$(a_{Nb})_{min}$, 1373 K	$(a_C)_{min}$, 1373 K	$(a_{Nb})_{min}$, 1573 K	$(a_C)_{min}$, 1573 K
50	6.21×10^{-6}	5.49×10^{-5}	2.86×10^{-5}	1.44×10^{-4}
49	↓	1.48×10^{-4}	↓	1.68×10^{-4}
48		5.56×10^{-4}		8.39×10^{-4}
46		3.93×10^{-3}		5.93×10^{-3}
44		0.011		0.017
42		.021		.031
40		.037		.056

TaC

Alloy composition, at %	$(a_{Ta})_{min}$, 1373 K	$(a_C)_{min}$, 1373 K	$(a_{Ta})_{min}$, 1573 K	$(a_C)_{min}$, 1573 K
50	4.48×10^{-6}	3.80×10^{-5}	2.27×10^{-5}	1.57×10^{-4}
49	↓	1.23×10^{-4}	↓	3.03×10^{-4}
48		2.11×10^{-4}		5.17×10^{-4}
46		4.05×10^{-4}		9.93×10^{-4}
44		5.78×10^{-4}		1.41×10^{-3}
40		8.63×10^{-4}		2.10×10^{-3}

Ta_2C

Alloy composition, at %	$(a_{Ta})_{min}$, 1373 K	$(a_C)_{min}$, 1373 K	$(a_{Ta})_{min}$, 1573 K	$(a_C)_{min}$, 1573 K
50	1.66×10^{-4}	2.22×10^{-6}	5.05×10^{-4}	1.43×10^{-5}
49	↓	2.26×10^{-5}	↓	5.34×10^{-5}
48		6.58×10^{-5}		1.55×10^{-4}
46		2.42×10^{-4}		5.74×10^{-4}
44		4.93×10^{-4}		1.16×10^{-3}
40		1.09×10^{-3}		2.58×10^{-3}

TiC

Alloy composition, at %	$(a_{Ti})_{min}$, 1373 K	$(a_C)_{min}$, 1373 K	$(a_{Ti})_{min}$, 1573 K	$(a_C)_{min}$, 1573 K
50	4.01×10^{-7}	6.18×10^{-7}	3.26×10^{-6}	4.15×10^{-6}
49	↓	1.97×10^{-6}	↓	8.00×10^{-6}
48		3.79×10^{-6}		1.37×10^{-5}
46		2.68×10^{-5}		5.85×10^{-5}
44		7.75×10^{-5}		1.69×10^{-4}
40		2.57×10^{-4}		5.58×10^{-4}

V_2C

Alloy composition, at %	$(a_V)_{min}$, 1373 K	$(a_C)_{min}$, 1373 K	$(a_V)_{min}$, 1573 K	$(a_C)_{min}$, 1573 K
40 - 50	1.84×10^{-3}	3.42×10^{-6}	4.2×10^{-3}	1.78×10^{-5}

VC

Alloy composition, at %	$(a_V)_{min}$, 1373 K	$(a_C)_{min}$, 1373 K	$(a_V)_{min}$, 1573 K	$(a_C)_{min}$, 1573 K
40 - 50	3.77×10^{-4}	3.77×10^{-4}	1.2×10^{-3}	1.2×10^{-3}

W_2C

Alloy composition, at %	$(a_W)_{min}$, 1373 K	$(a_C)_{min}$, 1373 K	$(a_W)_{min}$, 1573 K	$(a_C)_{min}$, 1573 K
40 - 50	0.025	6.36×10^{-4}	0.028	7.9×10^{-4}

WC

Alloy composition, at %	$(a_W)_{min}$, 1373 K	$(a_C)_{min}$, 1373 K	$(a_W)_{min}$, 1573 K	$(a_C)_{min}$, 1573 K
40 - 50	0.047	0.047	0.072	0.072

ZrC

Alloy composition, at %	$(a_{Zr})_{min}$, 1373 K	$(a_C)_{min}$, 1373 K	$(a_{Zr})_{min}$, 1573 K	$(a_C)_{min}$, 1573 K
50	1.00×10^{-7}	1.16×10^{-5}	9.14×10^{-7}	5.74×10^{-3}
48	↓	3.94×10^{-4}	↓	6.67×10^{-4}
46		3.87×10^{-3}		6.53×10^{-3}
44		0.013		0.022
40		.054		.091

CrB_2

Alloy composition, at %	$(a_{Cr})_{min}$, 1373 K	$(a_B)_{min}$, 1373 K	$(a_{Cr})_{min}$, 1573 K	$(a_B)_{min}$, 1573 K
50	7.13×10^{-4}	9.02×10^{-3}	1.98×10^{-3}	0.017
48	5.45×10^{-4}		5.03×10^{-3}	↓
46	7.40×10^{-3}	↓	0.068	
44	0.03		.282	

HfB_2

Alloy composition, at %	$(a_{Hf})_{min}$, 1373 K	$(a_B)_{min}$, 1373 K	$(a_{Hf})_{min}$, 1573 K	$(a_B)_{min}$, 1573 K
50	6.10×10^{-12}	6.14×10^{-6}	1.97×10^{-10}	1.15×10^{-5}
48	4.67×10^{-12}	5.24×10^{-5}	7.46×10^{-11}	1.46×10^{-4}
46	6.34×10^{-11}	1.64×10^{-4}	1.01×10^{-9}	4.57×10^{-4}
44	2.62×10^{-10}	3.04×10^{-4}	4.20×10^{-9}	8.51×10^{-4}
40	1.29×10^{-9}	6.13×10^{-4}	2.04×10^{-8}	1.70×10^{-3}

V_3B_2

Alloy composition, at %	$(a_V)_{min}$, 1373 K	$(a_B)_{min}$, 1373 K	$(a_V)_{min}$, 1573 K	$(a_B)_{min}$, 1573 K
50	4.49×10^{-4}	3.22×10^{-6}	1.27×10^{-3}	1.76×10^{-5}
49	4.22×10^{-4}	↓	1.23×10^{-3}	↓
48	4.11×10^{-4}		1.74×10^{-3}	
46	9.82×10^{-4}		4.15×10^{-3}	
44	1.57×10^{-3}		6.67×10^{-3}	
40	2.68×10^{-3}		0.011	

V_2B_3

Alloy composition, at %	$(a_V)_{min}$, 1373 K	$(a_B)_{min}$, 1373 K	$(a_V)_{min}$, 1573 K	$(a_B)_{min}$, 1573 K
50	3.60×10^{-6}	8.01×10^{-5}	2.02×10^{-5}	2.89×10^{-4}
49	3.12×10^{-6}	↓	1.87×10^{-5}	↓
48	2.93×10^{-6}		4.07×10^{-5}	
46	2.07×10^{-5}		2.87×10^{-4}	
44	6.01×10^{-5}		8.34×10^{-4}	
40	1.99×10^{-4}		2.74×10^{-3}	

ZrB_2

Alloy composition, at %	$(a_{Zr})_{min}$, 1373 K	$(a_B)_{min}$, 1373 K	$(a_{Zr})_{min}$, 1573 K	$(a_B)_{min}$, 1573 K
50	4.01×10^{-11}	1.62×10^{-5}	1.26×10^{-9}	1.12×10^{-4}
49	3.31×10^{-11}	5.43×10^{-5}	1.13×10^{-9}	1.56×10^{-4}
48	3.06×10^{-11}	1.38×10^{-4}	3.19×10^{-9}	3.83×10^{-4}
46	4.16×10^{-10}	4.33×10^{-4}	4.34×10^{-9}	1.20×10^{-3}
44	1.71×10^{-9}	8.05×10^{-4}	1.79×10^{-9}	2.23×10^{-3}
40	8.50×10^{-9}	1.62×10^{-3}	8.78×10^{-7}	4.47×10^{-3}

BeO

Alloy composition, at %	$(a_{Be})_{min}$, 1373 K	$(a_{Be})_{min}$, 1573 K
50	1.45×10^{-4}	4.24×10^{-4}
48	4.77×10^{-5}	1.95×10^{-4}
46	2.92×10^{-5}	1.19×10^{-4}
44	2.18×10^{-5}	8.94×10^{-5}
40	1.48×10^{-5}	6.10×10^{-5}

CaO

Alloy composition, at %	$(a_{Ca})_{min}$, 1373 K	$(a_{Ca})_{min}$, 1573 K
50	8.83×10^{-5}	3.31×10^{-4}
48	2.90×10^{-5}	1.53×10^{-4}
46	1.76×10^{-5}	9.27×10^{-5}
44	1.31×10^{-5}	6.93×10^{-5}
40	9.13×10^{-6}	4.77×10^{-5}

CeO_2

Alloy composition, at %	$(a_{Ce})_{min}$, 1373 K	$(a_{Ce})_{min}$, 1573 K
50	4.36×10^{-3}	9.22×10^{-3}
48	4.72×10^{-4}	1.93×10^{-3}
46	1.78×10^{-4}	7.21×10^{-4}

Gd_2O_3

Alloy composition, at %	$(a_{Gd})_{min}$, 1373 K	$(a_{Gd})_{min}$, 1573 K
50	1.75×10^{-6}	8.44×10^{-6}
49	5.61×10^{-7}	4.43×10^{-6}
48	3.31×10^{-7}	2.62×10^{-6}
46	1.58×10^{-7}	1.25×10^{-6}
44	1.02×10^{-7}	8.07×10^{-7}
40	5.82×10^{-8}	4.61×10^{-7}

HfO_2

Alloy composition, at %	$(a_{Hf})_{min}$, 1373 K	$(a_{Hf})_{min}$, 1573 K
50	3.38×10^{-5}	8.42×10^{-5}
48	3.65×10^{-6}	1.76×10^{-5}
46	1.37×10^{-6}	6.58×10^{-6}
44	7.62×10^{-7}	3.68×10^{-6}
40	3.60×10^{-7}	1.74×10^{-6}

La_2O_3

Alloy composition, at %	$(a_{Hf})_{min}$, 1373 K	$(a_{Hf})_{min}$, 1573 K
50	3.25×10^{-6}	1.27×10^{-5}
48	6.13×10^{-7}	4.44×10^{-6}
46	2.94×10^{-7}	1.87×10^{-6}
44	1.89×10^{-7}	1.21×10^{-6}
40	1.07×10^{-7}	6.94×10^{-7}

MgO

Alloy composition, at %	$(a_{Mg})_{min}$, 1373 K	$(P_{Mg})_{eq.}$, 1373 K	$(a_{Mg})_{min}$, 1573 K	$(P_{Mg})_{eq.}$, 1573 K
50	2.53×10^{-3}	3.55×10^{-3}	6.30×10^{-3}	0.038
48	8.41×10^{-4}	1.16×10^{-3}	2.87×10^{-3}	.017
46	5.11×10^{-4}	7.16×10^{-4}	1.76×10^{-3}	.01
44	3.81×10^{-4}	5.34×10^{-4}	1.31×10^{-3}	8.13×10^{-3}
40	2.64×10^{-4}	3.65×10^{-4}	9.10×10^{-4}	5.60×10^{-3}

Sc_2O_3

Alloy composition, at %	$(a_{Sc})_{min}$, 1373 K	$(a_{Sc})_{min}$, 1573 K
50	5.45×10^{-8}	4.34×10^{-7}
48	1.02×10^{-8}	1.34×10^{-7}
46	4.93×10^{-9}	6.42×10^{-8}
44	3.17×10^{-9}	4.15×10^{-8}
40	1.81×10^{-9}	2.37×10^{-8}

TiO

Alloy composition, at %	$(a_{Ti})_{min}$, 1373 K	$(a_{Ti})_{min}$, 1573 K
50	0.029	0.039
48	9.77×10^{-3}	.018
46	5.98×10^{-3}	.011
44	4.46×10^{-3}	8.36×10^{-3}
40	3.06×10^{-3}	5.75×10^{-3}

Y_2O_3

Alloy composition, at %	$(a_Y)_{min}$, 1373 K	$(a_Y)_{min}$, 1573 K
50	3.82×10^{-8}	2.92×10^{-7}
48	7.19×10^{-9}	9.05×10^{-8}
46	3.45×10^{-9}	4.32×10^{-8}
44	2.22×10^{-9}	2.79×10^{-8}
40	1.26×10^{-9}	1.59×10^{-8}

ZrO_2

Alloy composition, at %	$(a_{Zr})_{min}$, 1373 K	$(a_{Zr})_{min}$, 1573 K
50	3.28×10^{-8}	7.41×10^{-4}
48	3.54×10^{-5}	1.56×10^{-4}
46	1.33×10^{-5}	5.79×10^{-4}
44	7.40×10^{-6}	3.24×10^{-5}
40	3.50×10^{-6}	1.53×10^{-5}

BN

Alloy composition, at %	$(a_B)_{min}$, 1373 K	$(a_B)_{min}$, 1573 K
50	0.16	0.16
49	.05	.09
48	.03	.05
46	.01	.02
44	9.3×10^{-3}	.015
40	5.3×10^{-3}	9.0×10^{-3}

HfN

Alloy composition, at %	$(a_{Hf})_{min}$, 1373 K	$(a_{Hf})_{min}$, 1573 K
50	4.23×10^{-6}	1.54×10^{-5}
49	1.35×10^{-6}	8.14×10^{-6}
48	8.46×10^{-7}	4.80×10^{-6}
46	3.82×10^{-7}	2.29×10^{-6}
44	2.46×10^{-7}	1.48×10^{-6}
40	1.40×10^{-7}	8.46×10^{-7}

LaN

Alloy composition, at %	$(a_{La})_{min}$, 1373 K	$(a_{La})_{min}$, 1573 K
50	0.02	0.032
49	6.29×10^{-3}	.017
48	3.71×10^{-3}	.01
46	1.78×10^{-3}	4.79×10^{-3}
44	1.14×10^{-3}	3.10×10^{-3}
40	6.53×10^{-4}	1.77×10^{-3}

TaN

Alloy composition, at %	$(a_{Ta})_{min}$, 1373 K	$(a_{Ta})_{min}$, 1573 K
50	0.138	0.125
49	.044	.065
48	.026	.038
46	.012	.018
44	8.07×10^{-3}	.012
40	4.60×10^{-3}	6.83×10^{-3}

TiN

Alloy composition, at %	$(a_{Ti})_{min}$, 1373 K	$(a_{Ti})_{min}$, 1573 K
50	1.65×10^{-4}	4.37×10^{-4}
49	5.30×10^{-5}	2.29×10^{-4}
48	3.12×10^{-5}	1.35×10^{-4}
46	1.49×10^{-5}	6.46×10^{-5}
44	9.63×10^{-6}	4.18×10^{-5}
40	5.49×10^{-6}	2.39×10^{-5}

ZrN

Alloy composition, at %	$(a_{Zr})_{min}$, 1373 K	$(a_{Zr})_{min}$, 1573 K
50	1.42×10^{-5}	5.12×10^{-5}
49	4.54×10^{-6}	2.69×10^{-5}
48	2.68×10^{-6}	1.59×10^{-5}
46	1.28×10^{-6}	7.57×10^{-6}
44	8.27×10^{-7}	4.90×10^{-6}
40	4.71×10^{-7}	2.80×10^{-6}

Cr_3Si

Alloy composition, at %	$(a_{Cr})_{min}$, 1373 K	$(a_{Si})_{min}$, 1373 K	$(a_{Cr})_{min}$, 1573 K	$(a_{Si})_{min}$, 1573 K
50	0.208	1.30×10^{-4}	0.275	4.22×10^{-4}
49	.451	↓	.428	↓
48	.644		.611	
46	.995		.944	

Cr_5Si_3

Alloy composition, at %	$(a_{Cr})_{min}$, 1373 K	$(a_{Si})_{min}$, 1373 K	$(a_{Cr})_{min}$, 1573 K	$(a_{Si})_{min}$, 1573 K
50	0.183	8.57×10^{-4}	0.244	1.92×10^{-3}
49	.738	8.57×10^{-4}	.539	1.92×10^{-3}

Mo_3Si

Alloy composition, at %	$(a_{Mo})_{min}$, 1373 K	$(a_{Si})_{min}$, 1373 K	$(a_{Mo})_{min}$, 1573 K	$(a_{Si})_{min}$, 1573 K
50	0.134	7.44×10^{-5}	0.187	3.82×10^{-4}
49	.291	3.50×10^{-5}	.292	2.01×10^{-4}
48	.415	↓	.416	1.33×10^{-4}
46	.642		.643	↓
44	.813		.814	

Mo_5Si_3

Alloy composition, at %	$(a_{Mo})_{min}$, 1373 K	$(a_{Si})_{min}$, 1373 K	$(a_{Mo})_{min}$, 1573 K	$(a_{Si})_{min}$, 1573 K
50	0.046	1.33×10^{-4}	0.077	5.08×10^{-4}
49	.188	7.07×10^{-5}	.17	3.55×10^{-4}
48	.357	5.27×10^{-5}	.323	2.65×10^{-4}
46	.781	3.50×10^{-5}	.707	1.75×10^{-4}

Nb_5Si_3

Alloy composition, at %	$(a_{Nb})_{min}$, 1373 K	$(a_{Si})_{min}$, 1373 K	$(a_{Nb})_{min}$, 1573 K	$(a_{Si})_{min}$, 1573 K
50	0.014	1.12×10^{-6}	0.028	4.29×10^{-6}
49	.057	1.41×10^{-4}	.063	1.16×10^{-4}
48	.108	2.01×10^{-3}	.121	1.67×10^{-3}

Ta_2Si

Alloy composition, at %	$(a_{Ta})_{min}$, 1373 K	$(a_{Si})_{min}$, 1373 K	$(a_{Ta})_{min}$, 1573 K	$(a_{Si})_{min}$, 1573 K
50	0.027	1.31×10^{-3}	0.047	3.51×10^{-3}
49	.088	0.013	.091	0.013
48	.151	.038	.155	.038

Ta_5Si_3

Alloy composition, at %	$(a_{Ta})_{min}$, 1373 K	$(a_{Si})_{min}$, 1373 K	$(a_{Ta})_{min}$, 1573 K	$(a_{Si})_{min}$, 1573 K
50	0.026	1.76×10^{-3}	0.045	4.34×10^{-3}
49	.104	0.012	.099	0.013
48	.198	.029	.188	.031

Ti_5Si_3

Alloy composition, at %	$(a_{Ti})_{min}$, 1373 K	$(a_{Si})_{min}$, 1373 K	$(a_{Ti})_{min}$, 1573 K	$(a_{Si})_{min}$, 1573 K
50	4.15×10^{-4}	6.96×10^{-8}	1.27×10^{-3}	4.50×10^{-7}
49	1.67×10^{-3}	4.73×10^{-7}	2.80×10^{-3}	1.35×10^{-6}
48	3.16×10^{-3}	1.39×10^{-6}	5.33×10^{-3}	3.29×10^{-6}
46	6.92×10^{-3}	3.64×10^{-5}	0.011	3.69×10^{-5}

TiSi

Alloy composition, at %	$(a_{Ti})_{min}$, 1373 K	$(a_{Si})_{min}$, 1373 K	$(a_{Ti})_{min}$, 1573 K	$(a_{Si})_{min}$, 1573 K
50	8.53×10^{-4}	1.89×10^{-5}	2.65×10^{-3}	6.80×10^{-5}
49	8.67×10^{-3}	6.04×10^{-5}	9.92×10^{-3}	1.15×10^{-4}
48	0.025	1.15×10^{-4}	0.029	2.24×10^{-4}

V_3Si

Alloy composition, at %	$(a_V)_{min}$, 1373 K	$(a_{Si})_{min}$, 1373 K	$(a_V)_{min}$, 1573 K	$(a_{Si})_{min}$, 1573 K
50	0.065	3.96×10^{-6}	0.105	2.35×10^{-5}
49	.140	↓	.163	↓
48	.201		.233	
46	.311		.360	
44	.393		.457	
40	.513		.595	

V_5Si_3

Alloy composition, at %	$(a_V)_{min}$, 1373 K	$(a_{Si})_{min}$, 1373 K	$(a_V)_{min}$, 1573 K	$(a_{Si})_{min}$, 1573 K
50	1.48×10^{-3}	2.78×10^{-7}	2.88×10^{-3}	1.62×10^{-7}
49	5.95×10^{-3}	↓	6.37×10^{-3}	↓
48	0.011		0.012	
46	.024		.026	
44	.037		.04	
40	.061		.065	

Zr_2Si

Alloy composition, at %	$(a_{Zr})_{min}$, 1373 K	$(a_{Si})_{min}$, 1373 K	$(a_{Zr})_{min}$, 1573 K	$(a_{Si})_{min}$, 1573 K
50	9.44×10^{-4}	2.75×10^{-3}	3.76×10^{-5}	4.70×10^{-4}
49	3.01×10^{-3}	5.31×10^{-3}	4.73×10^{-3}	1.86×10^{-3}

Zr_5Si_3

Alloy composition, at %	$(a_{Zr})_{min}$, 1373 K	$(a_{Si})_{min}$, 1373 K	$(a_{Zr})_{min}$, 1573 K	$(a_{Si})_{min}$, 1573 K
50	5.31×10^{-4}	3.93×10^{-5}	1.70×10^{-3}	5.11×10^{-4}
49	2.14×10^{-3}	2.19×10^{-3}	3.75×10^{-3}	1.53×10^{-3}

ZrSi

Alloy composition, at %	$(a_{Zr})_{min}$, 1373 K	$(a_{Si})_{min}$, 1373 K	$(a_{Zr})_{min}$, 1573 K	$(a_{Si})_{min}$, 1573 K
50	1.19×10^{-4}	9.30×10^{-5}	5.22×10^{-4}	6.59×10^{-4}
49	1.21×10^{-3}	1.04×10^{-3}	1.95×10^{-3}	1.27×10^{-3}

APPENDIX E
COMPATIBILITY CALCULATIONS UTILIZING Be ACTIVITY DATA IN BERYLLIDES

Gibbs free energy of formation data for many Be-rich intermetallic compounds are not available. However, in a few cases, the activity of Be in these intermetallics have been measured and, as described below, these can be utilized to determine the compatibility of NiAl alloys with Be-rich intermetallic compounds.

For a system consisting of NiAl alloy phase and a Be-rich intermetallic phase, the compound NiBe can be formed provided the activity product $(a_{Ni})_{NiAl} \times (a_{Be})_{Be\text{-}rich}$ is greater than the reciprocal of the equilibrium constant for the reaction

$$\underline{Ni} + \underline{Be} = NiBe$$

where the underline denotes that the elements are present at reduced activity; $(a_{Ni})_{NiAl}$ is the activity of Ni in the NiAl phase; $(a_{Be})_{Be\text{-}rich}$ is the activity of Be in the Be-rich intermetallic phase. If the conditions are satisfied for precipitation of the NiBe compound, the alloy can be considered to be incompatible with the Be-rich intermetallic compound.

The compatibility of $Be_{13}La$, $Be_{12}Ta$, and $Be_{17}Ta_2$ with NiAl alloys have been determined by the above mentioned procedure. The following table gives the activities of Be in these compounds which were obtained from the compilations by Hultgren et al. (ref. 1):

Compound	Temperature of measurement, K	(a_{Be})
$Be_{13}La$	1400	0.33
$Be_{12}Ta$	1600	.31
$Be_{17}Ta_2$	1600	.31

REFERENCE FOR APPENDIX E

1. R. Hultgren, P. D. Desai, D. T. Hawkins, M. Gleiser, and K. K. Kelley, Selected Thermodynamic Properties of Binary Alloys", American Society of Metals, Metals Park, OH (1973).

NASA
National Aeronautics and Space Administration

Report Documentation Page

1. Report No.	2. Government Accession No.	3. Recipient's Catalog No.
NASA CR-4171		

4. Title and Subtitle

Thermodynamic Analysis of Compatibility of Several Reinforcement Materials With Beta Phase NiAl Alloys

5. Report Date

November 1988

6. Performing Organization Code

7. Author(s)

Ajay K. Misra

8. Performing Organization Report No.

None (E-4299)

10. Work Unit No.

535-07-01

9. Performing Organization Name and Address

Case Western Reserve University
10900 Euclid Avenue
Cleveland, Ohio 44106

11. Contract or Grant No.

NCC-3-43

13. Type of Report and Period Covered

Contractor Report
Final

12. Sponsoring Agency Name and Address

National Aeronautics and Space Administration
Lewis Research Center
Cleveland, Ohio 44135-3191

14. Sponsoring Agency Code

15. Supplementary Notes

Project Manager, Carl A. Stearns, Materials Division, NASA Lewis Research Center. Ajay K. Misra, NASA Resident Research Associate.

16. Abstract

Chemical compatibility of several reinforcement materials with beta phase NiAl alloys within the concentration range 40 to 50 at% Al have been analyzed from thermodynamic considerations at 1373 and 1573 K. The reinforcement materials considered in this study include carbides, borides, oxides, nitrides, beryllides, and silicides. Thermodynamic data for NiAl alloys have been reviewed and activity of Ni and Al in the beta phase have been derived at 1373 and 1573 K. Criteria for chemical compatibility between the reinforcement material and the matrix have been defined and several chemically compatible reinforcement materials have been identified.

17. Key Words (Suggested by Author(s))	18. Distribution Statement
Aluminides Fibers Compatibility Thermodynamics	Unclassified – Unlimited Subject Category 24

19. Security Classif. (of this report)	20. Security Classif. (of this page)	21. No of pages	22. Price*
Unclassified	Unclassified	60	A04

NASA FORM 1626 OCT 86

*For sale by the National Technical Information Service, Springfield, Virginia 22161

NASA-Langley, 1988

National Aeronautics and
Space Administration
Code NTT-4

Washington, D.C.
20546-0001

NASA

NASA SCIENTIFIC AND TECHNICAL DOCUMENT AVAILABILITY AUTHORIZATION (DAA)

To be initiated by the responsible NASA Project Officer, Technical Monitor, or other appropriate NASA official for all presentations, reports, papers, and proceedings that contain scientific and technical information. Explanations are on the back of this form and are presented in greater detail in NHB 2200.2, "NASA Scientific and Technical Information Handbook."

☒ Original
☐ Modified

(Facility Use Only)
Control No. _____
Date _____

I. DOCUMENT/PROJECT IDENTIFICATION (Information contained on report documentation page should not be repeated except title, date and contract number)

Title: _____

Author(s): _____

Originating NASA Organization: _____

Performing Organization (if different) _____

Contract/Grant/Interagency/Project Number(s) _____

Document Number(s) -4171 Document Date: _____

(For presentations or externally published documents, enter appropriate information on the intended publication such as name, place, and date of conference, periodical or journal title or book title and publisher: _____

These documents must be routed to NASA Headquarters, International Affairs Division for approval. (See Section VII))

II. AVAILABILITY CATEGORY

Check the appropriate category(ies).

Security Classification: ☐ Secret ☐ Secret RD ☐ Confidential ☐ Confidential RD ☒ Unclassified

Export Controlled Document - Documents marked in this block must be routed to NASA Headquarters International Affairs Division for approval.

☐ ITAR ☐ EAR

NASA Restricted Distribution Document

☐ FEDD ☐ Limited Distribution ☐ Special Conditions-See Section III

Document disclosing an invention

☐ Documents marked in this block must be withheld from release until six months have elapsed after submission of this form, unless a different release date is established by the appropriate counsel. (See Section IX).

Publicly Available Document

☐ Publicly available documents must be unclassified and may not be export-controlled or restricted distribution documents

☐ Copyrighted ☐ Not copyrighted

III. SPECIAL CONDITIONS

Check one or more of the applicable boxes in each of (a) and (b) as the basis for special restricted distribution if the "Special Conditions" box under NASA Restricted Distribution Document in Section II is checked. Guidelines are provided on reverse side of form.

a. This document contains:

☐ Foreign government information ☐ Commercial product test or evaluation results ☐ Preliminary information ☐ Information subject to special contract provision

☐ Other—Specify _____

b. Check one of the following limitations as appropriate:

☐ U.S. Government agencies and U.S. Government agency contractors only ☐ NASA contractors and U.S. Government agencies only ☐ U.S. Government agencies only

☐ NASA personnel and NASA contractors only ☐ NASA personnel only ☐ Available only with approval of issuing office: _____

IV. BLANKET RELEASE (OPTIONAL)

All documents issued under the following contract/grant/project number _____ may be processed as checked in Sections II and III.

The blanket release authorization granted _____ (Date) is:

☐ Rescinded - Future documents must have indivdual availability authorizations. ☐ Modified - Limitations for all documents processed in the STI system under the blanket release should be changed to conform to blocks as checked in Section II.

V. PROJECT OFFICER/TECHNICAL MONITOR

Typed Name of Project Officer/Technical Monitor	Office Code	Signature	Date
_____	2C	_____	_____

VI. PROGRAM OFFICE REVIEW ☐ Approved ☐ Not Approved

Typed Name of Program Office Representative	Program Office and Code	Signature	Date
_____	_____	_____	_____

VII. INTERNATIONAL AFFAIRS DIVISION REVIEW

☐ Open, domestic conference presentation approved. ☐ Export controlled limitation is not applicable.

☐ Foreign publication/presentation approved. ☐ The following Export controlled limitation (ITAR/EAR) is assigned to this document: _____

☐ Export controlled limitation is approved.

International Affairs Div. Representative	Title	Date
_____	_____	_____

VIII. EXPIRATION OF REVIEW TIME

The document is being released in accordance with the availability category and limitation checked in Section II since no objection was received from the Program Office within 20 days of submission, as specified by NHB 2200.2, and approval by the International Affairs Division is not required.

Name & Title Sue Reilly Office Code 540. Date 7/2/88

Note: This release procedure cannot be used with documents designated as Export Controlled Documents, conference presentations or foreign publications.

IX. DOCUMENTS DISCLOSING AN INVENTION

a. This document may be released on _____ (Date) Installation Patent or Intellectual Property Counsel _____ Date _____

b. The document was processed on _____ (Date) in accordance with Sections II and III as applicable. NASA STI Facility _____ Date _____

X. DISPOSITION

Completed forms should be forwarded to the **NASA Scientific and Technical Information Facility, P.O. Box 8757, B.W.I. Airport, Maryland 21240**, with either (check box):

☐ Printed or reproducible copy of document enclosed.

☐ Abstract or Report Documentation Page enclosed. The issuing or sponsoring NASA installation should provide a copy of the document, when complete, to the NASA Scientific and Technical Information Facility at the above listed address.

FF427 REV OCT86